

# TRANSPORT IN LOW-DIMENSIONAL INTERACTING SYSTEMS

A Dissertation  
Presented to  
The Academic Faculty

By

Kamal Sharma

In Partial Fulfillment  
of the Requirements for the Degree  
Doctor of Philosophy in the  
School of Physics

Georgia Institute of Technology

December 2019

Copyright © Kamal Sharma 2019

# TRANSPORT IN LOW-DIMENSIONAL INTERACTING SYSTEMS

Approved by:

Professor Michael Pustilnik, Advisor  
School of Physics  
*Georgia Institute of Technology*

Professor Andrew Zangwill  
School of Physics  
*Georgia Institute of Technology*

Professor Markus Kindermann  
School of Physics  
*Georgia Institute of Technology*

Professor Dragomir Davidovic  
School of Physics  
*Georgia Institute of Technology*

Professor Federico Bonetto  
School of Mathematics  
*Georgia Institute of Technology*

Date Approved: November 5, 2019

There's a lot of things you need to get across this universe. Warp drive. Wormhole refractors. You know the thing you need most of all? You need a hand to hold.

—*The 11<sup>th</sup> Doctor*

To Mummy Papa, To Akash, To Soumya.

## ACKNOWLEDGEMENTS

First and foremost, I would like to thank my advisor, Prof. Michael Pustilnik. I am very grateful for his guidance throughout my time working with him and could not have finished this journey without his support and confidence in me. Michael has inspired me to think simply and provided exactly the kind of hands-off approach I needed to learn and explore the field that I knew very little about.

I would also like to thank Prof. Andrew Zangwill, Prof. Markus Kindermann, Prof. Dragomir Davidovic and Prof. Federico Bonetto who graciously accepted to be the faculty advisors on my thesis committee. Their feedback, especially during the final semester of my Ph.D. and their suggestions during my defense has been very valuable in understanding the relevance of my work in the scientific arena.

I am also very fortunate to know Prof. Brian Kennedy who taught me two amazing courses on graduate-level Quantum Mechanics. Prof. Kennedy has always been someone whom I have admired as a physicist and a teacher. He has inspired me to take pride in whatever I do and be respectful towards everyone around me. I am very thankful for all the times he has taken out time to help me when I was stuck on a research problem. He never made me feel judged even when I went to him with the silliest of problems. Prof. Flavio Fenton has been another source of moral support. He is one of the best mentors that I have seen in graduate school and, to me, serves as an example of a physicist committed to research and towards development of his students as a future scientist.

My first ever Physics advisor Late Prof. Narendra Kumar brought about the biggest turning point in my academic life by taking me under his wing as my research advisor at Raman Research Institute. Without him, I would have never stepped into a Ph.D. program in Physics. I give my heartfelt thanks and respect to him.

I would have never completed this dissertation without the help of my wife, Soumya. Her unconditional love, sharp intellect and a truly funny sense of humor has kept me cheer-

ful even in the stressful periods of my research. She has played the role of a much needed fellow scientist and have helped me immensely in my development as a student of Physics. I cannot be more grateful to have her in my life and to have taken care of me when I needed it the most.

A Ph.D. is an arduous task for a novice graduate student and I could not have completed it without the support of my family. My parents Harimohan Sharma and Manju Sharma have always given me the freedom to explore and supported my decision to quit my job and pursue a Ph.D. in Physics. I also want to thank my newfound parents, Anand Mohan and Ranjana Mohan, who have always inspired me to be the best I can. I also want to thank my brother Akash who has always been the partner-in-mischief and one of biggest supporter all these years, and my sisters Shubhi and Pooja who are the youngest of the family and always bring levity and joy to my life.

Last but certainly not the least, I would like to thank the School of Physics at Georgia Tech for supporting me as a graduate student all these years. I am very grateful to the faculty and staff who have always strived to provide an open and nurturing environment for graduate students.

## TABLE OF CONTENTS

<b>Acknowledgments</b> . . . . .	v
<b>List of Tables</b> . . . . .	xi
<b>List of Figures</b> . . . . .	xii
<b>Chapter 1: Introduction</b> . . . . .	1
1.1 Historical background . . . . .	1
1.2 Transport in one-dimension . . . . .	3
1.2.1 The Wiedemann-Franz law . . . . .	3
1.2.2 Transport in Luttinger liquids . . . . .	4
1.2.3 Violation of the Wiedemann-Franz law: Real quantum wires . . . . .	5
1.2.4 Backscattering changes transport coefficients . . . . .	5
1.3 What's different about one-dimension? . . . . .	6
1.4 Models for one-dimensional interacting systems . . . . .	7
1.4.1 Bethe Ansatz (1931) . . . . .	7
1.4.2 Tomonaga (1950) and Luttinger (1963) . . . . .	7
1.4.3 Mattis and Lieb (1965) . . . . .	10
1.4.4 Haldane (1980s) . . . . .	10
1.5 Role of interaction: Electron liquids and Wigner crystals . . . . .	11

1.6	Physical realization of one-dimensional Wigner crystal . . . . .	12
1.6.1	Suspended carbon nanotubes . . . . .	13
1.7	Wigner crystal in one-dimension . . . . .	13
1.7.1	Experimental evidence of interaction and non-integrability . . . . .	17
1.8	Applications and technology . . . . .	18
<b>Chapter 2: Models of interacting quantum particles: A brief overview . . . . .</b>		<b>19</b>
2.1	Physics of interacting quantum particles . . . . .	19
2.2	Interacting particles in higher dimensions: . . . . .	20
2.2.1	Adiabatic continuity in higher dimensions . . . . .	22
2.2.2	Properties of quasiparticles . . . . .	25
2.3	Excitations of one-dimensional electrons . . . . .	26
2.4	Bosonic excitations: Road to the solution . . . . .	27
2.5	Solution of the Tomonaga-Luttinger (TL) model: Brief review . . . . .	28
2.5.1	The Hamiltonian . . . . .	28
2.5.2	Bosonization . . . . .	29
2.6	Generalization of one-dimensional interacting particles: The Luttinger liquid conjecture . . . . .	32
2.7	Inadequacy of the Tomonaga-Luttinger model and Luttinger liquid theory . . . . .	33
<b>Chapter 3: Beyond Luttinger liquid: curved dispersion . . . . .</b>		<b>35</b>
3.1	Failure of perturbation theory: Decay of linear bosons . . . . .	35
3.2	Fermionic description: Dynamic structure factor . . . . .	37
3.2.1	Linear spinless fermions (Tomonaga-Luttinger model) . . . . .	38

3.2.2	Free spinless fermions . . . . .	39
3.2.3	Weakly interacting fermions . . . . .	40
<b>Chapter 4: Calculations . . . . .</b>		<b>43</b>
4.1	Wigner crystal . . . . .	43
4.1.1	The Harmonic approximation: Phonons . . . . .	45
4.2	Wigner crystal as Luttinger liquid . . . . .	46
4.3	Ballistic thermal conductance: Harmonic Wigner crystal . . . . .	47
4.4	Anharmonic perturbations: Interaction between phonons . . . . .	52
4.5	Scattering processes in Wigner crystal . . . . .	53
4.5.1	The Umklapp process . . . . .	53
4.5.2	Non-Umklapp processes . . . . .	54
4.6	Model of our setup: inhomogeneous Luttinger liquid . . . . .	54
4.6.1	Eigenfunctions and eigenvalues . . . . .	55
4.7	Correction to thermal conductance . . . . .	57
4.7.1	Collision integral . . . . .	57
4.8	Approximations and calculation of $\mathcal{A}$ and $W$ . . . . .	60
4.8.1	Parametrically small momentum transfer . . . . .	60
4.8.2	Bose Factors $\mathcal{A}_{q,p;q_1,q_2}$ : Linear response in $\delta T$ . . . . .	61
4.8.3	Scattering probability $W_{q,p;q_1,q_2}$ . . . . .	67
4.9	Artifacts of our model and how to eliminate them . . . . .	70
4.9.1	Result . . . . .	76
<b>Chapter 5: Results and Discussion . . . . .</b>		<b>77</b>

5.1	Correction to thermal conductance . . . . .	78
5.2	Fate of Wiedemann-Franz law . . . . .	79
5.2.1	Applicability to integral models . . . . .	80
5.2.2	Screened Coulomb interaction . . . . .	80
5.2.3	Comparison with weakly interacting electrons . . . . .	81
<b>Appendix A: Integrals . . . . .</b>		<b>84</b>
<b>References . . . . .</b>		<b>93</b>
<b>Vita . . . . .</b>		<b>94</b>

## LIST OF TABLES

- 4.1 Bose factors for all possible combinations (left column) of reservoirs (Right/Left) of origin of phonons. The phonons have been labeled by their wave numbers  $q, p, q_1, q_2$ . . . . . 62
- 4.2 Table showing calculated  $c$  and  $d$  factors to be used in the integrals for correction to thermal conductance. . . . . 68

## LIST OF FIGURES

1.1	Quantized conductance in multiples of $e^2/\pi\hbar$ of ballistic point contact measured in GaAs-AlGaAs heterostructure.[5] . . . . .	2
1.2	A simplified schematic of one-dimensional quantum wire made from 2DEG device. . . . .	3
1.3	Marbles are confined to move in one dimension. Kinetic energy imparted to any of the marbles gets distributed to other marbles due to inevitable collisions. This leads to a collective motion of marbles. . . . .	6
1.4	Sin-Itiro Tomonaga . . . . .	8
1.5	Free electron dispersion (solid) vs Tomonaga model (dashed) vs Luttinger liquid (dotted) . . . . .	10
1.6	(a) two-dimensional optical lattice, giving rise to 1dWG, (b) three-dimensional optical lattice forming a lattice of neutral atoms. . . . .	12
1.7	(a) Scanning electron microscope image of a suspended carbon nanotube, (b) Schematic of the experiment in [51] . . . . .	13
1.8	Schematic of a GaAs-AlGaAs heterostructure. Two-dimensional electron gas layer is constricted using two contacts. . . . .	14
1.9	Dependence of the ratio of the kinetic and potential energies on the density $\rho_0$ for a screened Coulomb interaction. In a typical quantum wire system, the Bohr radius $a_B$ is much smaller than the distance $d$ to the capacitively coupled gate electrode. In the Wigner crystal regime $E_{kin}/E_{int} \ll 1$ . . . . .	15
1.10	Comparison between excitations of a one-dimensional system (right) and a higher dimensional system (right) . . . . .	18
2.1	Fermi-Dirac probability distribution. . . . .	22

2.2	Visual illustration of a quasiparticle [79] . . . . .	22
2.3	(a) Probability distribution of free fermions (Fermi-Dirac distribution) and (b) for a Fermi liquid with $Z_k$ discontinuity. Spectral function of (c) fermi gas vs (d) Fermi liquid . . . . .	24
2.4	Comparison between excitations of a one-dimensional system (right) and a higher dimensional system (left) . . . . .	26
2.5	Excitation spectrum for a generic one-dimensional Fermi system (left) and corresponding excitation spectrum for the Tomonaga-Luttinger model for $m \rightarrow \infty$ (right). Low energy excitations become sharply defined under the TL approximation. . . . .	27
3.1	Structure factor for Tomonaga-Luttinger model. . . . .	38
3.2	Structure factor of free one-dimensional fermions. . . . .	40
3.3	Wigner crystal phonons under linear approximation (Luttinger liquid), weak non-linearity $\xi$ , and exact harmonic dispersion. . . . .	41
3.4	(a) Linear dispersion of an ideal Luttinger liquid. The decay of a phonon (filled circle) with wave number $q$ into two phonons (hollow circles) with wavenumber $q'_1$ and $q'_2$ is allowed under energy and momentum conser- vation but diverges. (b) A non-linearity in the dispersion (3.12) allows a minimum of two phonons each in both initial and final state of a scattering event. . . . .	42
4.1	Wigner crystal in one-dimension . . . . .	44
4.2	Ballistic phonon transport between boson reservoirs. . . . .	48
4.3	Scattering events redistribute the flow of energy and leads to a correction to thermal conductance . . . . .	49
4.4	Phonon dispersion relation for harmonic Wigner crystal (solid) and lin- earized low temperature approximation (dashed). . . . .	50
4.5	Setting up the problem - one-dimensional Wigner crystal, leads and reservoirs	58

4.6	(a) A linear dispersion leads to divergences in perturbation theory in interaction for a three phonon process. It also forbids decay of one phonon into two phonons due to violation of energy and momentum conservations. (b) Curvature in the dispersion relation conserves net momentum and energy for a 2 – 2 processes and resolves the mentioned divergence. . . . .	58
4.7	Three possible cases of scattering pairs that conserve momentum and energy. These scattering processes contribute to $\delta j_E$ . . . . .	61
4.8	An example of a process for case I for inhomogeneous electron density. Phonons $q, p, q_1, q_2$ originating from L,L,L and R reservoir respectively. . .	63
4.9	[Averaging over the oscillations of a function.]An illustrative figure showing how our <i>averaging</i> eliminates the oscillations (solid line) due to sharp potential step. We desire the mean behavior (dotted) of this function. . . .	71

## SUMMARY

We study the fate of Wiedemann-Franz law in one-dimensional spinless electrons. Luttinger liquid theory describes low-energy excitations of a gapless one-dimensional many-body system. We go beyond the assumptions of the Luttinger liquid theory to get the properties of real one-dimensional systems. Chapter 1 gives an introduction and background of the state of research in one-dimensional systems and discusses the Wigner crystal. Chapter 2 covers a brief review of the theoretical methods to study one-dimensional systems including Fermi liquid theory and various one-dimensional models and methods. It also discusses the violation of the famous Wiedemann-Franz law and why the conventional theories fail to explain thermalization of such systems. We introduce the new paradigm of extending these models to beyond Luttinger liquid framework such that they can be used to describe the phenomena that were missing. We specifically work on a perturbative calculation of the correction to thermal conductance of a Wigner crystal wire in chapter 4 by considering interaction and non-linear dispersion in a Wigner crystal. We then discuss our results and the fate of Wiedemann-Franz law in chapter 5. We end with a brief discussion of possible future work in chapter 5.

# CHAPTER 1

## INTRODUCTION

### 1.1 Historical background

Physicists have been fascinated with one-dimensional quantum many-body systems for more than 90 years now. From the traditional classical physics perspective, a one-dimensional model for a problem used to serve as a gateway to complex higher dimensional “*real systems*.” It was believed that since our world is three-dimensional, any physical system can only be described completely only in a three-dimensional framework. Study of one-dimensional systems used to be a theoretical exercise towards gaining insight in solving three-dimensional problems. This philosophy, however, has been proven to be inaccurate with the discovery of low-dimensional materials that show very rich and complicated behaviors. Today, one-dimensional and two-dimensional physical systems are just as real as everyday three-dimensional objects.

A low-dimensional system is the result of confinement of particles, living in three-dimensional space, by an external potential. For example, a two-dimensional electron gas device, commonly abbreviated as 2DEG, is a *heterogeneous semiconductor junction* of two similarly doped (*p-p type* or *n-n type*) semiconductor materials [1, 2, 3, 4]. The most commonly used 2DEG device is a GaAs layer sandwiched between two AlGaAs layers as shown in Figure 1.8. This leads to the formation of a layer of mobile electrons between the two parallel interfaces of AlGaAs layers. Under appropriate voltage this layer of electrons can be made essentially two-dimensional. Moreover, the same device can be modified to apply additional confinement to the two-dimensional electron gas such that it becomes a one-dimensional electron system.

The first experiment that showed a conclusive signature of a one-dimensional electron

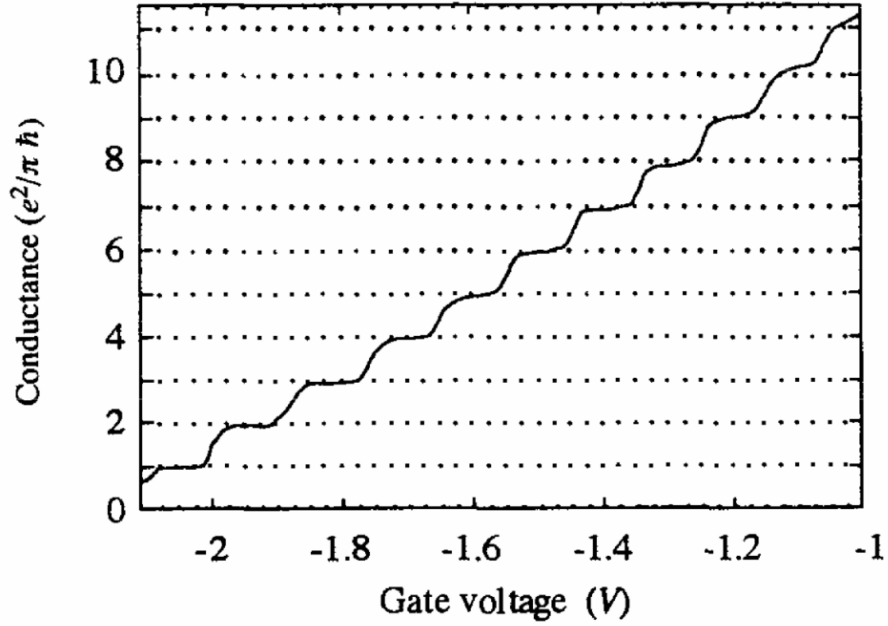


Figure 1.1: Quantized conductance in multiples of  $e^2/\pi\hbar$  of ballistic point contact measured in GaAs-AlGaAs heterostructure.[5]

system was conducted by van Wees *et al.* and Wharam *et al.* [5, 6]. The experiment measured electrical conductance of a narrow constriction, called a *quantum point contact*, QPC, created by confining a two-dimensional electron gas by an external potential. This historic observation showed a striking phenomenon known as *conductance quantization* as shown in the plot of gate voltage versus conductance, refer Figure 1.1. The plot shows essentially constant conductance between regular points where it increases in steps of universal conductance quantum

$$\text{Conductance Quantization} \quad G_0 = e^2/\pi\hbar, \quad (1.1)$$

where  $e$  is the charge of an electron and  $\hbar$  is the *Planck's constant*.

Figure 1.2 illustrates the experimental setup used for the aforementioned experiment. Metallic gates (green) on either side of the GaAs-AlGaAs heterostructure device are charged with a negative voltage. As a result, they repel the electrons and essentially squeeze the

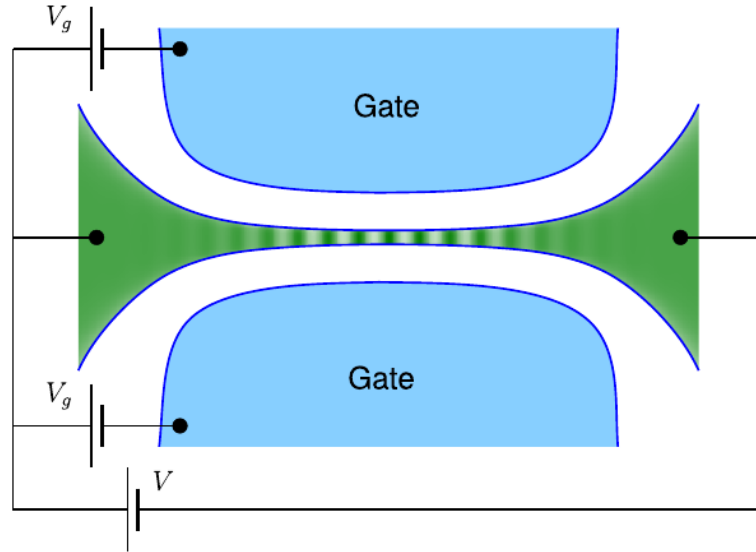


Figure 1.2: Confinement of a 2DEG (green) by metallic gates (blue) renders the transport one-dimensional. Electrons in this channel are one-dimensional and have low enough density to form a Wigner crystal. However, the density increases away from the center and periodic order is washed out by quantum fluctuations.

two-dimensional electron gas (blue) into a single narrow channel. However, the thickness of the electron gas is not uniform. It is wider near the terminals but converges to a narrow one-dimensional channel in the center. Although the length of this one-dimensional region is negligible compared to the whole device, any current passing through this setup is forced to pass through the narrow constriction and thus has a component of the conductance of the one-dimensional constriction. Moreover, the quantized nature of the conductance plot also indicates that the transport in this system is basically one-dimensional.

## 1.2 Transport in one-dimension

### 1.2.1 The Wiedemann-Franz law

In 1853, Gustav Wiedemann and Rudolph Franz quantified the well-known phenomenon that metals that are good conductors of electricity turn out to be good thermal conductors as well. They stated that the ratio of thermal conductivity ( $K$ ) to electrical conductivity ( $G$ )

at the same temperature is roughly the same for all metals:

$$K = \pi^2 GT / 3e^2 \quad (1.2)$$

where,  $k_B = 1$  in energy units. This relationship, known as the Wiedemann-Franz law, is a natural property of systems in which thermal energy and charge both are carried by electron excitations. The quantum of electrical conductance  $G_0$  equation (1.1) and thermal conductance  $K_0$  also satisfy the Wiedemann-Franz law:

$$K_0 = \frac{2\pi^2 T}{3\hbar}. \quad (1.3)$$

It has been shown that this relation is satisfied in the presence of elastic scattering of electrons with impurities and crystal vibrations (phonons) [7] if there is no interaction between electrons. However, in the presence of electron-electron interaction, i.e., Fermi liquids in two and three dimensions, the Wiedemann-Franz law breaks down [8, 9]. This is because the inelastic scattering processes lead to different corrections to thermal and electrical conductance. Thus, violation of the Wiedemann-Franz law is a signature of electron-electron interaction effects and is of considerable experimental and theoretical interest.

### 1.2.2 Transport in Luttinger liquids

The interactions between electrons have a much stronger effect on the physics of the system in one-dimension as compared to higher dimensions. However, Fermi liquid theory fails in more than one way [10, 11], in one dimension as discussed in chapter (2). The most general mathematical description of one-dimensional interacting electrons is the Luttinger liquid theory [11], refer section (1.4.2). Theoretical study of conductance properties of ideal and isolated Luttinger liquid quantum wire models has shown no effect on the quantum of either electrical conductance  $G_0$  [12, 13, 14] or the thermal conductance  $K_0$  [15]. Therefore, an ideal Luttinger liquid conductor satisfies the Wiedemann-Franz law.

### 1.2.3 Violation of the Wiedemann-Franz law: Real quantum wires

In recent years, much of the research on one-dimensional quantum wires has been focused on the phenomena not explained by the Luttinger liquid theory [16, 17, 18, 19]. Equilibration of a one-dimensional electron liquid [20] is one such effect which requires scattering between the energy carrying excitations in one-dimension. Another example is the phenomena of Coulomb drag [21]. Here a current carrying quantum wire induces a voltage across a another quantum wire close to it. This voltage is induced due to interaction between the electrons in two wires when there is an absence of particle-hole symmetry which requires a curved dispersion of excitations.

### 1.2.4 Backscattering changes transport coefficients

When the Luttinger liquid is non-ideal, the above conclusion does not hold. For example, Kane and Fischer [22] showed that the presence of very weak impurity inside a Luttinger liquid induces backscattering of electrons. Backscattering of carriers redistribute the energy and momentum currents and lead to new renormalized electrical ( $G$ ) and thermal ( $K$ ) conductance. This leads to violation of the Wiedemann-Franz law.

Another such example is the Luttinger liquid with inhomogeneities on long length scales [15]. The electrons participating in any dynamic process in a fermi system at low temperature are the ones that lie close to the Fermi surface (Fermi points in one dimension). Since the deBroglie wavelength of these electrons is much smaller than the length scale of the inhomogeneity, they see the slowly varying potential as an adiabatic change in potential and thus do not suffer backscattering. However, momentum conservation does not hold because of broken translational symmetry of space. Long wavelength (low energy) collective excitations see this inhomogeneity as sharp changes and thus have a finite amplitude of reflection and transmission in the wire. Therefore, a part of the energy current changes direction due to backscattering. The thermal conductance  $K$  is thus renormalized in this case while the electrical conductance  $G$  remains unchanged.

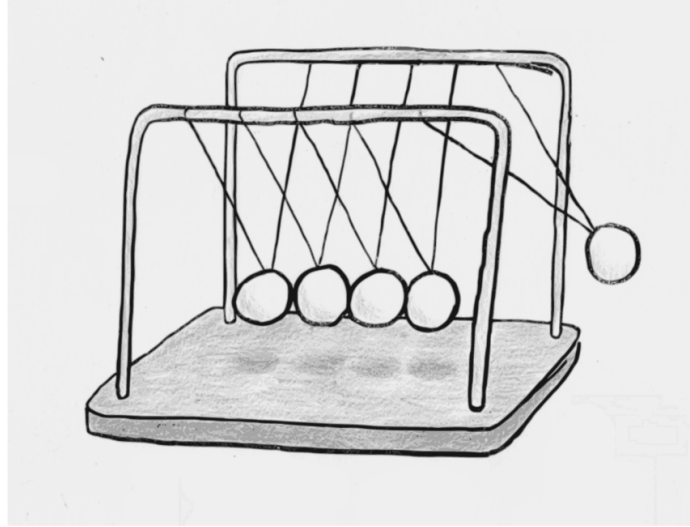


Figure 1.3: Marbles are confined to move in one dimension. Kinetic energy imparted to any of the marbles gets distributed to other marbles due to inevitable collisions. This leads to a collective motion of marbles.

### 1.3 What's different about one-dimension?

The most important aspect of confining the fermions to one dimension is that they cannot move past each other. A simple analogy to one-dimensional systems is the well-known *Newton's cradle*, see Figure 1.3, in which marbles are constrained by the threads to move in one-dimension. It is very intuitive to see that it is impossible to have any individual marble in motion without affecting the rest of the marbles. In fact, even if we choose to start the system by moving one marble, it quickly manifests in collective motion of many marbles.

Similarly, for a system of many particles, any energy given to the system manifests in the form of collective excitation of a large number of particles. In higher dimensions, the excitations of a many-particle system resemble single-particle excitations of some non-interacting system. Traditional approaches like the perturbation theory for weak interaction and the Fermi liquid theory [23] for strongly interacting fermions have been very successful in describing the behavior of electron systems in two and three dimensions. However, the physics of particles in one-dimension even with arbitrarily weak interactions is qualitatively

different from their higher dimensional counterparts [24, 11]. This is because interactions play a key role in one-dimensional systems. As a result, even a weak interaction between particles can dramatically change the physics of a one-dimensional system. The excitations of a one-dimensional system are more complicated than non-interacting quasiparticles and need a different theoretical approach towards understanding their properties. Therefore, a novel approach that is non-perturbative in nature was needed.

## 1.4 Models for one-dimensional interacting systems

### 1.4.1 Bethe Ansatz (1931)

One of the first approaches was used by Hans Bethe to study the Heisenberg model [11], a one-dimensional lattice of quantum spins. In 1930s, Hans Bethe gave an elegant solution [25], that starts from a microscopic description of the spin chain and yields very accurate energy spectra for the ground and excited states. This method came to be known as the *Bethe-ansatz* and has since been developed as a powerful tool with a wider applicability for lattice and continuum systems, especially in the case of gapped spectrum. Unfortunately, the wavefunctions calculated using *Bethe-ansatz* tend to have a complicated form and using them to derive the operators and correlation functions is a formidable task.

### 1.4.2 Tomonaga (1950) and Luttinger (1963)

A non-perturbative method for one-dimensional fermions was first used by Tomonaga [26] in his model of electrons with linearized dispersion (1950). Luttinger, who was unaware of the existence of Tomonaga's model proposed a slightly different model [27] in 1956.

#### *Tomonaga's Model*

In 1950, Tomonaga came up with a profound method that seemed to tackle one-dimensional fermions. He used Bloch's method of sound waves [28, 29] for a many fermion problem in one-dimension. Bloch's assertion as quoted from Tomonaga's abstract [26] is as follows:



Figure 1.4: Sin-Itiro Tomonaga

*The fact implied by Bloch several years ago that in some approximate sense the behavior of an assembly of Fermi particles can be described by a quantized field of sound waves in the Fermi gas, where the sound field obeys Bose statistics. . . –Tomonaga,1950.*

It was this insight that inspired Tomonaga to study this assertion in mathematical detail in the case of an assembly of Fermi particles. This equivalence eventually culminated in the form of modern *Bosonization* [30] method that forms the bedrock of strongly interacting one-dimensional systems and strongly correlated quantum systems.

Tomonaga considered the high-density limit of interacting fermions in one dimension. In this regime, the Fourier transform of the two-body interaction potential is non-zero only for small wave numbers, i.e.,  $|k| \leq k_c$ , where the cut-off threshold,  $k_c$ , is much smaller than the Fermi momentum, i.e.,

$$k_c \ll k_F.$$

This implies that the ground state of the system contains a small number of particle excitations far above the Fermi surface and a small number of holes deep inside the Fermi sea:

$$|k| - k_F \ll k_c.$$

Since the relevant physics involves only the electrons near the two Fermi points (Fermi surface in one dimension), the electron dispersion can be linearized (1.5) near the Fermi level  $k = \pm k_F$ :

$$\varepsilon = \varepsilon_F \pm v_F(k \mp k_F). \quad (1.4)$$

The next crucial step was to define the density operator and the realization that it can be split into right-moving and left-moving components. The derivation presented in [26] leads to a quadratic form Hamiltonian in creation/annihilation operators and a linear excitation dispersion.

However, Tomonaga's model falls short in the presence of interaction between the bosonic excitations of the model. Such interactions, as we will see, lead to divergent relaxation rates and thus cannot explain thermalization of the electron system.

### *Luttinger Model*

After Tomonaga, Luttinger independently developed his own model for a one-dimensional electron gas in which he treated spinless and massless (in relativistic sense where  $c \longleftrightarrow v_F$ ) fermions. The basic difference between this model and Tomonaga's model was that now the linear branches of the spectrum were extended to negative infinite energies as well, Figure 1.5. In addition to that, he also included the interaction between the fermions that were moving in the same direction and neglected the interaction between left and right moving fermions. According to his treatment, even the smallest amount of interaction destroys the discontinuity of the Fermi surface in one dimension [27].

$$\langle n_{k,+} \rangle - \frac{1}{2} \sim \left| \frac{k - k_F}{k_c} \right|^{\alpha_L} \text{sign}(k_F - k), \quad (1.5)$$

where  $\alpha_L$ , called the anomalous dimension, depends on the interaction strength.

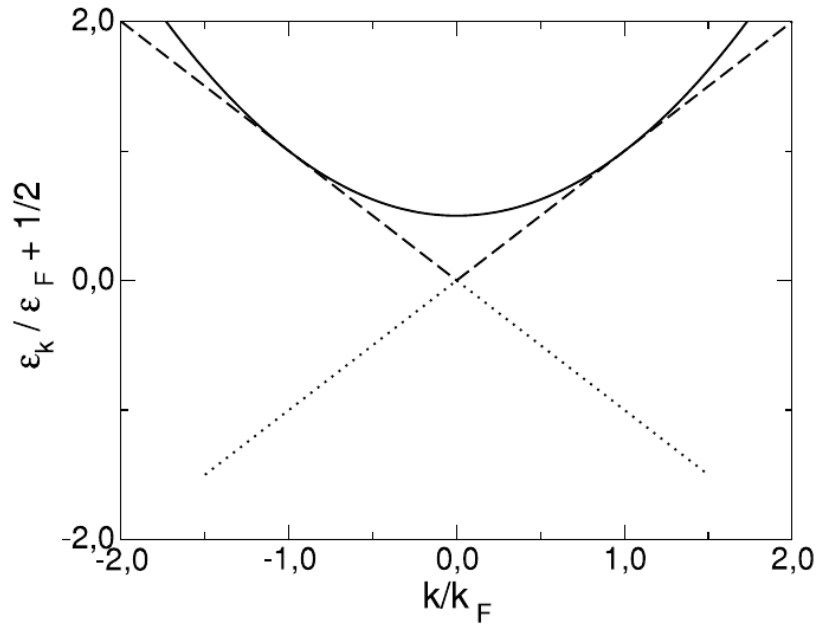


Figure 1.5: Free electron dispersion (solid) vs Tomonaga model (dashed) vs Luttinger liquid (dotted)

#### 1.4.3 Mattis and Lieb (1965)

Luttinger's model was later found to have mathematical inconsistencies [31] and the first mathematically complete solution was constructed in 1965 by Mattis & Lieb [32].

#### 1.4.4 Haldane (1980s)

The Tomonaga-Luttinger model was later exactly solved and generalized as the universality class of one-dimensional interacting particles now known as "Luttinger liquids" [33, 34, 35]. The 1970s and 1980s experienced rapid progress in the development of theoretical tools in this field. It was around this time that technological progress in fabrication of isolated one-dimensional nanostructures and emergence of new materials opened doors for experimental investigation.

## 1.5 Role of interaction: Electron liquids and Wigner crystals

In a one-dimensional quantum wire, electrons repel each other via Coulomb forces. The strength of the interaction can be characterized by typical kinetic energy of an electron which is of the order of the Fermi energy,

$$E_F \sim \hbar^2 n^2 / m.$$

The typical interaction energy is of the order of  $e^2 n / \kappa_D$ , where  $n$  is electron density,  $m$  is the electron mass,  $\kappa_D$  is the dielectric constant of the material.

The properties of a many-electron system depend on these two scales of energies. When the density of particles is high, the kinetic energy dominates the total energy of the system. In such a situation the system is said to be in *weakly interacting* regime. A high kinetic energy means that the particles are travelling very fast and almost do not see the minima of interaction energy. The behavior of such a system is like a gas or a liquid of particles.

On the other extreme, is the case of a low electron density, i.e.,

$$\rho a_B \ll 1, \tag{1.6}$$

where,  $a_B = \hbar^2 \kappa / m e^2$  is the Bohr radius. Since the total energy is dominated by electron-electron interaction, to zeroth approximation, the system settles in the lowest interaction energy configuration. The electrons thus settle into the minima of interaction energy. The system is then said to be in the *strongly interacting* regime. The minimal energy configuration of this system is a crystalline state of equidistant electrons, called a Wigner crystal (see Figure 1.9) [36, 37].

Although the short-range order for a Wigner crystal is quite robust, for a classical model the long-range order disappears at any finite temperature due to thermal agitation. Moreover, in a quantum Wigner crystal, the quantum zero-point motion destroys the long-range

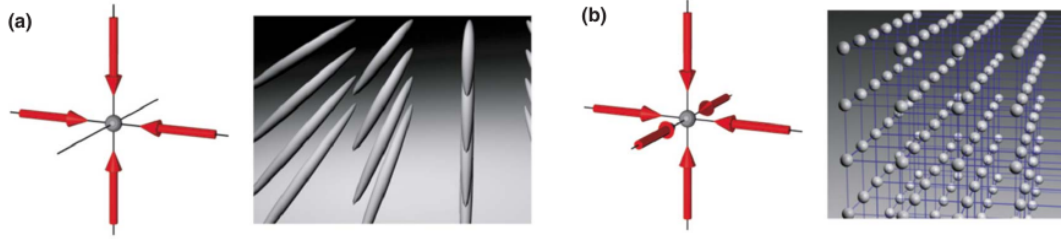


Figure 1.6: (a) two-dimensional optical lattice, giving rise to 1dWG, (b) three-dimensional optical lattice forming a lattice of neutral atoms.

order even at absolute zero [38]. However, the average distance between any two neighbors stays close to

$$\rho \sim 1/\rho_0,$$

where  $\rho_0$  is the particle density.

## 1.6 Physical realization of one-dimensional Wigner crystal

### *Ultracold Dipolar Gases in Trapped Atomic Lattices*

Both fermionic and bosonic one-dimensional Wigner crystals can be realized by confining ultra-cold dipolar quantum gases [39] in one-dimensional traps [40]. One-dimensional traps are essentially two-dimensional optical lattices constructed by superposition of two sets of counter propagating laser beams. If the confining potentials are deep enough and at ultra-cold temperatures, neutral atoms (bosonic or fermionic) [41, 42] are tightly confined along a narrow tube and are effectively free to move along the longitudinal direction [43, 44]. Review of many-body ultracold gases can be found at [40].

We will focus on the conductance of a one-dimensional Wigner crystal and the corrections to the conductance due to interactions present in the system.

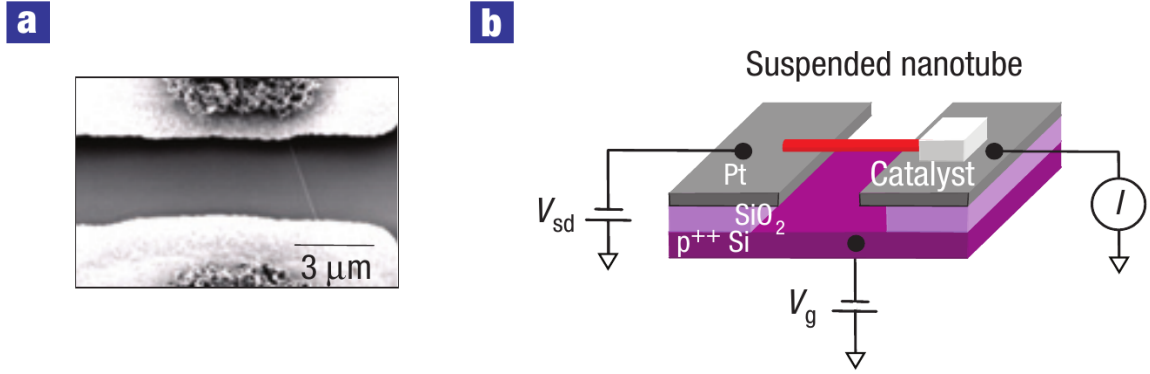


Figure 1.7: (a) Scanning electron microscope image of a suspended carbon nanotube, (b) Schematic of the experiment in [51]

### 1.6.1 Suspended carbon nanotubes

The one-dimensional Wigner crystal is expected to show magnetic and spin properties that are absent in the usual Luttinger liquid picture outside the Wigner crystal regime. Signature of Luttinger liquids for arbitrarily weak interactions have been observed experimentally in metallic and semiconductor based experiments [45, 46, 47, 48, 49, 50].

Carbon nanotubes are relatively clean high-mobility systems that can serve as a testing bed for the theory and has a promise for new technologies. The signature of a one-dimensional Wigner crystal formed by the hole gas in semi-conducting carbon nanotubes have been observed by Deshpande and Bockrath [51] using low temperature single electron transport spectroscopy in 2008. This was possible due to fabrication procedure by [52] where the disorder is controlled by growing carbon nanotubes while being suspended over the substrate and metallic contacts, see Figure 1.7.

## 1.7 Wigner crystal in one-dimension

A year after Deshpande *et al.*, Hew *et al.* observed the initial stages of formation one-dimensional Wigner crystal in quantum wires formed by confining a two-dimensional depleted electron gas in a GaAs/AlGaAs semiconducting heterostructure [53].

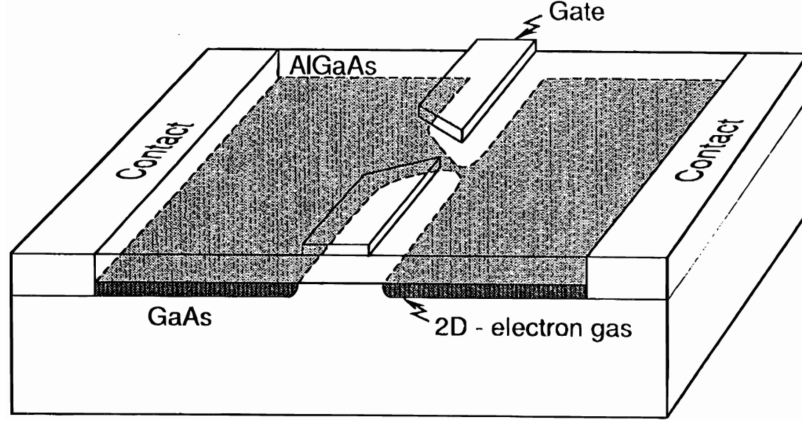


Figure 1.8: Schematic of a GaAs-AlGaAs heterostructure. Two-dimensional electron gas layer is constricted using two contacts.

In an experimental setup for measurements done on Wigner crystals, the presence of metallic gates surrounding the electron gas leads to an effective screening due to the image charges in the metallic gates. The screened Coulomb interaction takes the form:

$$V(x) = \frac{e^2}{\kappa} \left( \frac{1}{|x|} - \frac{1}{\sqrt{x^2 + (2d)^2}} \right), \quad (1.7)$$

where  $d$  is the distance of the quantum wire from the metallic gates. This means that for long distances the screening leads to a faster decay of interaction potential by a factor of  $2d^2/x^2 \ll 1$ . This implies that as  $\rho_0 \rightarrow 0$ , the order will be washed out by quantum fluctuations. We don't have to worry about  $\rho_0$  being so small because a comparison of the Fermi energy with the screened Coulomb interaction gives a Wigner crystal regime in the region:

$$a_B d^{-2} \ll \rho_0 \ll a_B^{-1} \ln(d/a_B), \quad (1.8)$$

where, the gate distance stays much larger than the Bohr radius

$$d \gg a_B.$$

A typical experiment involving GaAs devices have  $a_B \sim 10nm$  and gate distance  $d \gg$

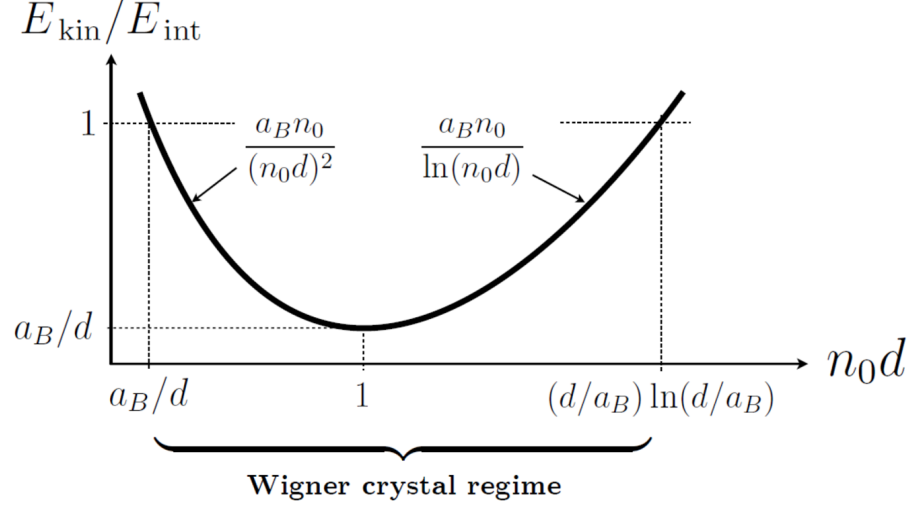


Figure 1.9: Dependence of the ratio of the kinetic and potential energies on the density  $\rho_0$  for a screened Coulomb interaction. In a typical quantum wire system, the Bohr radius  $a_B$  is much smaller than the distance  $d$  to the capacitively coupled gate electrode. In the Wigner crystal regime  $E_{kin}/E_{int} \ll 1$ .

100nm, thus ensuring spatial order. Only an extremely low density of the order of  $10^{-3}nm^{-1}$  will compromise the spatial order of the electrons. It can be seen that the ratio  $E_{kin}/E_{int}$  is a non-monotonic function of the density  $\rho_0$  as shown in Figure 1.9. The minimum of this plot occurs at  $E_{kin}/E_{int} \sim a_B/d \ll 1$ . The velocity  $v$  characterizing the low energy excitations (sound velocity) can be obtained using the thermodynamic relation:

$$v^2 = (\rho_0/m) \frac{d^2}{d\rho_0^2} (\rho_0 E_{GS}), \quad (1.9)$$

For the Wigner crystal where energy  $E_{GS} \approx E_{int} \sim e^2 \rho_0 / \kappa_D$ , the screening can be neglected for the limit where  $\rho_0 d \gg 1$ . This gives the sound velocity to be:

$$v \sim (e^2 \rho_0 / \kappa_D m)^{-1/2}, \quad (1.10)$$

where  $\kappa_D$  is the dielectric constant. These excitations are waves of density. In the case of crystals, such waves are called *phonons*. We will use the term *bosons, density waves*

or *phonons* to mean excitations of a Wigner crystal. The classical equations also predict the same sound velocity for low energy excitations. However, this does not mean that low-energy excitations of a Wigner crystal are classical in nature. The semi-classical description breaks down at low energies as shown in [54, 55, 56, 57, 58, 59, 60, 61]. Semi-classical treatment of a Wigner crystal can be used when the classical oscillations of the electrons about their mean position is larger than the amplitude,  $\delta x$ , of their quantum zero-point motion. For our one-dimensional case this amplitude,  $\delta x \sim \rho_0^{-1}(E_{kin}/E_{int})^{-1/4}$ , is small compared to the lattice spacing,  $\delta x \ll 1/\rho_0$ . This condition ensures not just that the ground state will have a robust short-range order. There is, therefore, a classical-to-quantum crossover region as the energy is lowered [61, 60].

The thermal and electrical properties of macroscopic systems are statistical manifestations of the equilibrium and transport of their constituent particles and their interaction with each other. A key factor that governs the physics of a system is its *dimensionality*, which usually emerges due to constraints on the physical dimensions. Even at the macroscopic scale, quantum mechanics determines properties of bulk matter, e.g., thermal and electrical conductivity, specific heat, refractive index, thermal expansion, etc. The role of quantum mechanics becomes more important when the characteristic length of a system is comparable to the de Broglie wavelength of its constituents. A one-dimensional quantum wire is one such system in which electrons are confined in the transverse directions but are free to move in the longitudinal one. Another example of a confined system is a quantum dot which is confined along all three spatial directions.

While the properties of many-body quantum systems are affected by the interaction between particles in higher dimensions, interactions play a special role in the properties of one-dimensional systems. These properties are direct consequences of the effect of interactions on correlations functions which are power-law functions. In mesoscopic devices and applied systems of quasi one-dimensional fermions, the interaction can be approximated as short-ranged owing to screening of the interaction due to neighboring linear chains.

Detailed studies of such systems have been conducted on a continuum “g-ology” model by [62, 63] and one-dimensional Hubbard Model [62, 64, 65].

However, isolated systems exhibit long-range Coulomb interaction of the form

$$V(r) \sim 1/r$$

due to the absence of neighboring chains. Signatures of isolated one-dimensional quantum wire phonons were first observed through resonant inelastic light-scattering experiments done on GaAs/AlGaAs heterostructures [66]. The phonon modes observed showed a linear dispersion relation owing to very weak coupling between quantum wires. Later, Schulz used the method of bosonization [62, 63] to show that long-range Coulomb interaction, even with a weak interaction strength, results in quasi long-range order [38]. Thus, one-dimensional fermions with long-range interaction resemble a Wigner crystal more than a continuum electron liquid.

### 1.7.1 Experimental evidence of interaction and non-integrability

Advancements in fabrication technology has led to availability of high mobility tunable constrictions that can be used to study very sensitive thermal measurements in two-dimensional electron gas (2DEG). These experiments have demonstrated the effects of interactions in one-dimensional quantum systems. Thermal transport experiments [67, 68] on isolated single channel quantum wires have shown a violation of Wiedemann-Franz law. In these studies, a reduced thermal conductance in contrast to the value predicted by Wiedemann-Franz law was measured at the plateau of electrical conductance. In other experiments, measurements on low-density quantum wires [69, 70] and quantum Hall-edge state systems [71] have shown an enhanced thermopower. An evidence of broken integrability was observed in experiments using momentum-resolved tunneling spectroscopy in the form of very clear thermalization in one-dimensional quantum wire [72, 73, 74]. These ob-

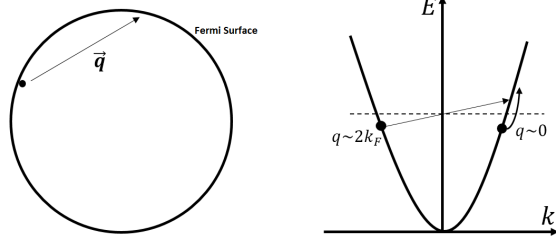


Figure 1.10: Comparison between excitations of a one-dimensional system (right) and a higher dimensional system (left)

Observations are inconsistent with the conventional Luttinger liquid theory and clearly point towards the existence of interactions in one-dimensional quantum systems.

## 1.8 Applications and technology

In experiments conducted on carbon nanotubes [51], the exchange coupling for a rarefied Wigner crystal state (separation  $\sim 100nm$ ) can be tuned individually using local gates. The spin lifetimes for carbon are much longer than traditional semiconductors which makes it a potential candidate for realization of a spin-based quantum bit (*qubit*).

## CHAPTER 2

### MODELS OF INTERACTING QUANTUM PARTICLES: A BRIEF OVERVIEW

Thermodynamic and transport properties of two-dimensional and three-dimensional systems of electrons have been studied under varying degrees of approximation [75, 76] from non-interacting to strongly interacting electrons. Landau Fermi liquid theory [23] and its subsequent development was a breakthrough in studying interacting electrons in two and three dimensions [77]. Landau's Fermi liquid theory is out of the scope of this work. However, a brief summary of Landau's quasiparticles and an understanding of its failure in one-dimension is instructive in motivating the study of one-dimensional systems.

#### 2.1 Physics of interacting quantum particles

Fermions are particles that obey Pauli exclusion principle which means that no two fermions can occupy the same single particle quantum state. At absolute zero, a non-interacting one-dimensional Fermi gas, has its energy states completely occupied up to a maximum energy level called the Fermi energy level. There is a sharp separation between these states and the unoccupied states above the Fermi level. As the temperature is raised, a small number of particles transition from states below the Fermi level to the higher unoccupied states leaving a hole behind. These *particle-hole excitations* live in a small neighborhood near the Fermi level. This state can serve as the zeroth order approximation to interacting electron system. In the case of non-interacting electrons, there is essentially no difference between the physics of one, two and three dimensions [78].

However, introduction of a weak interaction between Fermions excites a relatively large number of particles and holes but these are still confined in a narrow region near the Fermi points. At this point, the quantum state of the system is made up of the sum of amplitudes of the zeroth order state and the excited states. Increasingly stronger interaction excites

larger number of particles to very high energies far from the Fermi surface. This adds a very large amplitude of high energy particle-hole excitations to the zeroth order state. It follows that perturbation theory in strong interaction cannot be employed as the states of a real system are too different from the zeroth order state. Therefore, there was a need to develop new non-perturbative methods.

## 2.2 Interacting particles in higher dimensions:

An interacting many-body system can be adequately described by its ground state and the excitations of the system. The concept of quasiparticles forms the very core of our understanding of interacting quantum particles. The idea was first brought forward by Landau in the context of interacting fermion gas (fermion liquid) where quasiparticles make up for a simpler and more effective description of thermodynamic and transport properties. We first give a brief summary of Landau's quasiparticles and then associate that idea with excitations in one dimension.

A many particle quantum system is convenient to treat in the language of second quantization. The Hamiltonian of a many-particle system in the absence of an external potential can be written as:

$$\hat{H} = \sum_{ij} a_i^\dagger \hat{T}_{ij} a_j + \frac{1}{2} \sum_{ijkl} a_i^\dagger a_j^\dagger \hat{V}_{ijkl} a_k a_l, \quad (2.1)$$

with the statistics of the particles represented as commutation/anti-commutation relations  $[a_i, a_j] = \delta_{i,j}$  for bosons and  $\{a_i, a_j\} = \delta_{i,j}$  for fermions. For non-interacting particles, the inter-particle interaction  $V(r_1, r_2)$  is zero and the Hamiltonian becomes:

$$\hat{H} = \sum_{ij} a_i^\dagger \hat{T}_{ij} a_j.$$

The system of non-interacting particles can be constructed by solution of a single free

particle. The time independent Schrodinger equation for a free particle is:

$$-\frac{\hbar^2}{2m} \frac{\partial \psi(\mathbf{r})}{\partial \vec{r}} = E \psi(\mathbf{r}). \quad (2.2)$$

This can be solved using a periodic boundary condition  $\psi(\mathbf{r} + \vec{L}) = \psi(\mathbf{r})$  on a three-dimensional box with a volume  $V = L_x L_y L_z$ , where  $\vec{L} = (L_x, L_y, L_z)$  which gives us the following eigenstates and eigenvalues:

$$\psi_{\mathbf{k}}(\mathbf{r}) = \frac{e^{i\mathbf{k} \cdot \mathbf{r}}}{\sqrt{L_x L_y L_z}} = \frac{e^{i\mathbf{k} \cdot \mathbf{r}}}{\sqrt{V}}, \quad E_{\mathbf{k}} = \frac{\hbar^2 k^2}{2m}. \quad (2.3)$$

Here,  $k^2$  is written in terms of the cartesian components of  $\mathbf{k}$ ,  $k_j = \frac{2\pi n_j}{L_j}$  for  $j \in \{x, y, z\}$ .

For a system with a large number of electrons, Pauli's exclusion principle forbids any two electrons to be in the same state. Thus, at 0 K, electrons occupy all the lowest available energy states starting from  $k = 0$ . The energy of the highest occupied state is called the Fermi energy or Fermi level. The occupation number,  $n(\mathbf{k})$ , of state with momentum  $\hbar\mathbf{k} = \theta(k - k_F)$  suffers a discontinuity of unit amplitude at the Fermi surface. A system of volume  $V$  with  $N$  electrons and a density  $\rho = N/V$  has a Fermi energy of

$$E_F = \frac{\hbar^2}{2m} \left( \frac{3\pi^2 N}{V} \right)^{2/3} = \frac{\hbar^2}{2m} (3\pi^2 \rho)^{2/3}.$$

In contrast with the previous section's fictitious electrons without spin or interaction (free), real electrons have 1/2-spin and interact with each other via the long-range Coulomb interaction. Several modifications and increasingly accurate approximations to the free electron Hamiltonian have been devised to realistically model interacting electrons.

When the interactions are weak as compared to the kinetic energy of particles, for example in case of high-density electron gas, perturbation theory has been successfully employed. The independent electron picture acknowledges the presence of other electrons

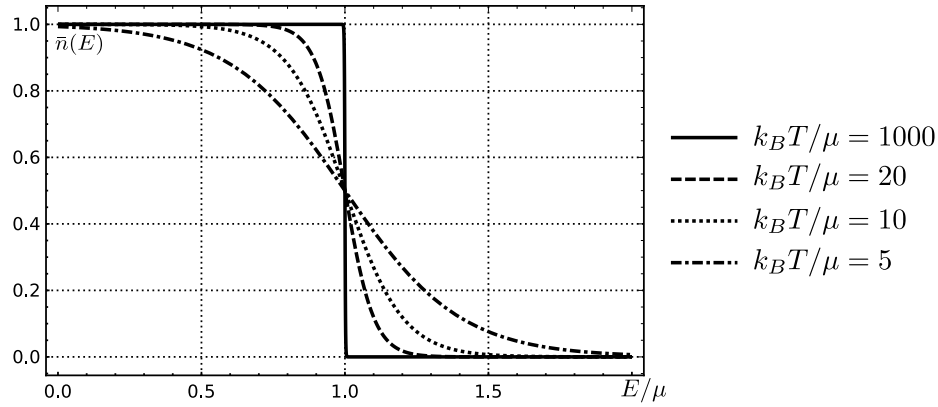


Figure 2.1: Fermi-Dirac probability distribution for a single fermion. The unit discontinuity at  $T = 0K$  gets smeared out over an energy range  $\sim k_B T$  at any non-zero temperature.

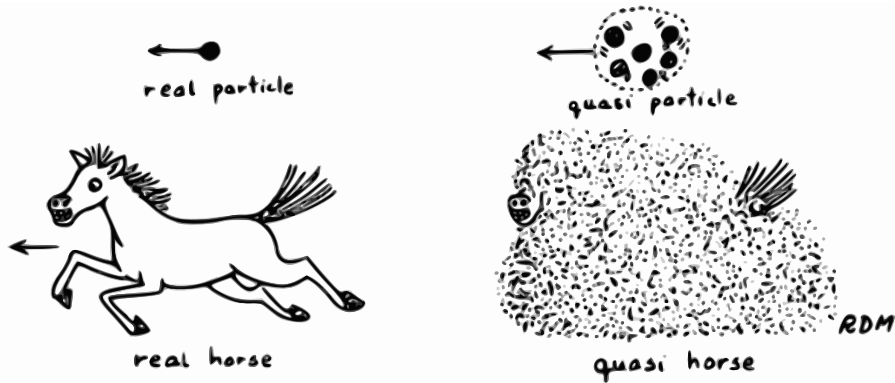


Figure 2.2: Visual illustration of a quasiparticle [79]

in the system and models that as screening of interaction potential. One would expect that in case of strong interactions, the free electron or independent electron picture will break down and the properties of the system will be drastically different than that of a non-interacting system.

### 2.2.1 Adiabatic continuity in higher dimensions

However, it was observed that even a strongly interacting fermi-gas ('Fermi-liquid') gave unexpectedly good results if treated as a gas of non-interacting particles. While Landau agreed that single particle wavefunctions in such a system will be very different from the free model, he argued that the agreement of such an interacting model with the non-

interacting model pointed towards existence of ‘something’ free/independent in the interacting system. He postulated that when the interactions are turned-on slowly the non-interacting fermionic single particle states transform smoothly into states of the interacting system. Thus, the states of the interacting system have a one-to-one correspondence with the single particle states in a non-interacting system. He named these ‘*quasiparticles*’, which can be physically understood as the particle along with a region of its influence (electron density cloud) on its neighborhood. For example, in electrodynamics, the electron *dresses* itself in a cloud of photons. In many-body systems, the bare particles surround themselves with particle-hole excitations of the ground state.

*What does the interaction change?*

The non-interacting Fermi gas at *zero temperature* has a unit discontinuity in the occupation number at the Fermi momentum. Further, the spectral function  $A(\omega, k)$  for a fermi gas is a delta function with zero width. The width of a peak in  $A(\omega, k)$  is proportional to  $1/\tau$ , where  $\tau$  is the typical lifetime of the excitation. A zero width of the peak implies that the excitations have infinite lifetimes, Figure 2.3. One would naively expect that as the interaction is turned on, some fermions will be pushed out of the Fermi sphere and lead to a smooth diffused boundary at  $\mathbf{k} = \mathbf{k}_F$ . On the contrary, the distribution maintains a sharp boundary at  $\mathbf{k} = \mathbf{k}_F$  with a discontinuity of size  $Z_k$ , Figure 2.3. This discontinuity only gets smoothed at non-zero temperatures.

Figure 2.2 shows an imaginative illustration sketched by Mattuck in his book “*A Guide to Feynman Diagrams in the Many-Body Problem*” [79]. The image shows a horse running through a dusty terrain with a cloud of dust travelling with it. Any given dust particle does not travel with the horse for too long but there is always a cloud made out new particles leaving behind old ones. If the *real horse* is like a bare particle, for example the electron, gas atoms etc., the dust cloud that has a sustained presence, is a direct consequence of interaction of the horse with its environment. Such a *quasi-horse* serves as a very good

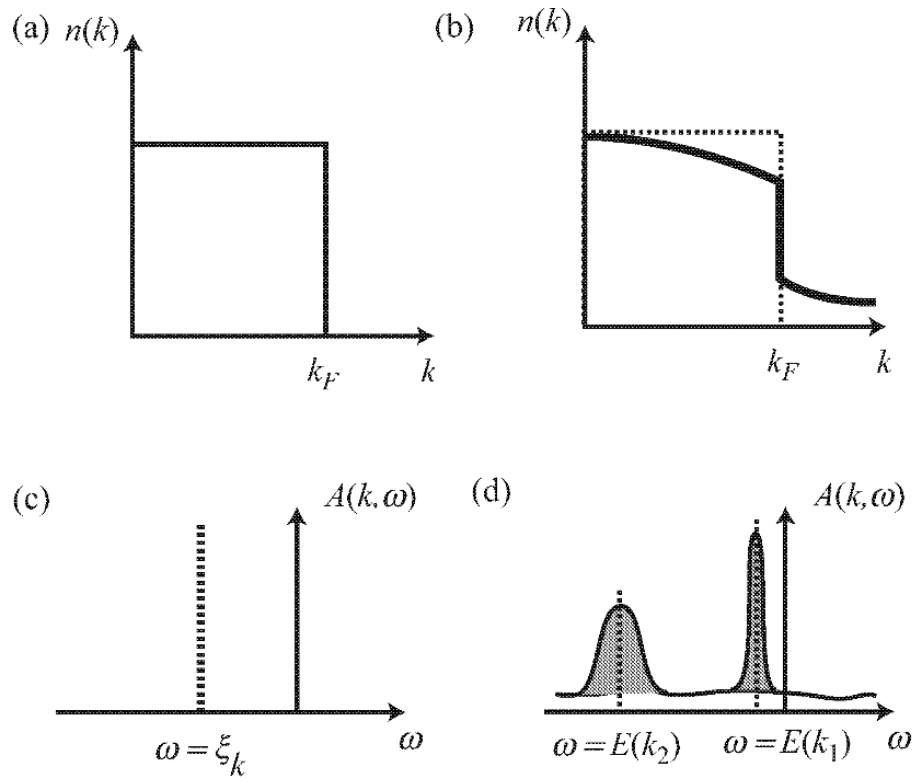


Figure 2.3: (a) Probability distribution of free fermions (Fermi-Dirac distribution) and (b) for a Fermi liquid with  $Z_k$  discontinuity. Spectral function of (c) fermi gas vs (d) Fermi liquid

analogy for the quasiparticle that is formed due to the influence of a bare particle on its environment. The quasi-particle contains the particle interaction effects within itself. The model thus emerges as a non-interacting or weakly interacting model of quasi-particles which can be studied using conventional methods including perturbation theory.

### 2.2.2 Properties of quasiparticles

Landau quasiparticles share the same charge and spin as those of ‘bare particles’ but have a different mass than the bare particles called the *effective mass*. Further, since they are dressed by density-fluctuations which are bosonic, the quasiparticles have the same spin-statistics as that of bare particles. As discussed before, the quasiparticles are either free or interact very weakly with each other. The weak interaction causes decay and scattering of quasiparticles. The amplitude of scattering can be calculated using Fermi Golden rule, but Landau used a more general phase-space argument for a simpler and intuitive description. A quasiparticle with momentum  $\mathbf{k}_1$  in the vicinity of the Fermi surface can scatter off another quasiparticle with momentum  $\mathbf{k}_2$ . Energy and momentum conservation restrict the momentum  $k_2$  of the other quasiparticle to lie in a phase space volume  $\sim (\epsilon - \epsilon_F)^2$ . The average lifetime,  $\tau$ , of a quasiparticle excitation goes as:

$$\tau \sim (\epsilon - \epsilon_F)^{-2}, \quad (2.4)$$

Therefore, the volume of phase space available to a quasiparticle for a scattering process vanishes at the Fermi surface. Such states have infinite lifetimes. However, away from the Fermi surface, the quasiparticles decay and thus are not exact eigenstates. They are long-lived but not stationary as the quasiparticles can scatter in and out of the states present in a thin band near the Fermi surface.

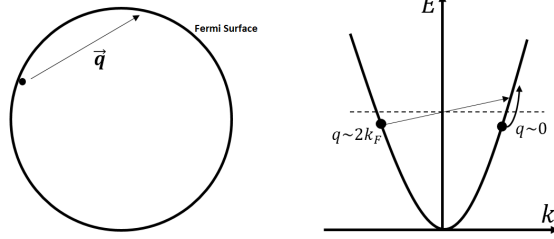


Figure 2.4: Comparison between excitations of a one-dimensional system (right) and a higher dimensional system (left)

### 2.3 Excitations of one-dimensional electrons

Unlike the Fermi liquid in higher dimensions, a one-dimensional electron system does not have stable quasi-particles when interactions are turned on. An elementary excitation forms when an electron is removed from below the Fermi level and placed at an energy level higher than the Fermi level. This creates a hole in the Fermi sea and a particle above it, hence the name *particle-hole excitation*. Considering such a particle with  $k < k_F$  promoted to  $k' = k + q > k_F$  leads to an excitation with well-defined momentum  $k' - k = q$ . Typically, the energy of such an excitation will depend on both  $\vec{k}$  and  $\vec{q}$ . In higher dimensions,  $k$  and  $q$  can always be selected anywhere on the Fermi surface, (Figure 2.4), which is a circle and a sphere in one and two spatial dimensions respectively. This leads to a continuous range for allowed momenta,  $q \in [0, 2k_F]$ , for collective excitations near the Fermi surface. However, in one dimension the Fermi surface is reduced to two points,  $k = \pm k_F$ , which means that particle-hole excitations exist only for  $q$  values close to 0 or  $2k_F$ . By expanding the quadratic dispersion for electrons ( $\xi(k) = k^2/(2m)$ ) near the Fermi points, the excitation energy spectrum can be calculated from  $E_k(q) = \xi(k) - \xi(k - q)$ . For a fixed excitation momentum  $q$ , there exists a continuum of states (see Figure 2.5) lying between

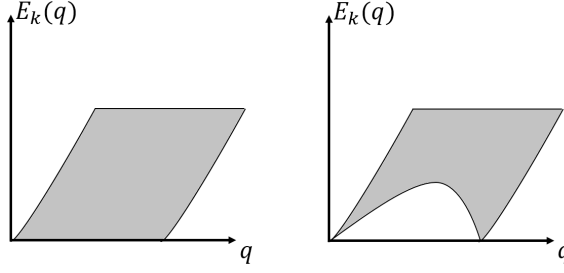


Figure 2.5: Excitation spectrum for a generic one-dimensional Fermi system (left) and corresponding excitation spectrum for the Tomonaga-Luttinger model for  $m \rightarrow \infty$  (right). Low energy excitations become sharply defined under the TL approximation.

the maximum and minimum of  $E_k(q)$  as:

$$v_F q - \frac{q^2}{2m} < E(q) < v_F q + \frac{q^2}{2m} \quad (2.5)$$

$$\delta E(q) = \max\{E_k(q)\} - \min\{E_k(q)\} = \frac{q^2}{m}, \quad (2.6)$$

where we have substituted  $k/m$  by  $v_F = k_F/m$  for small  $q$ . Here  $1/m$  is like the interaction constant in Fermi liquid theory. Excitations for the Tomonaga-Luttinger model are obtained as we linearize the free electron dispersion with respect to the two Fermi points and let the mass  $m \rightarrow \infty$  while keeping  $v_F$  constant. As a result,  $\delta E(q)$  goes to zero and the excitation energy becomes independent of free particle momentum  $k$ .

$$\left. \begin{array}{l} E(q) = v_F q \\ \delta E(q) = 0 \end{array} \right\} \text{low energy TL excitations.} \quad (2.7)$$

## 2.4 Bosonic excitations: Road to the solution

The energy of an excitation in one dimension *near the Fermi points* depends only on its momentum  $q$  and that both energy and momentum are well-defined. Furthermore,  $\delta E(q)$  in one dimension decays faster than  $E(q)$  similar to the quasiparticles in higher dimensional Fermi liquids. It follows that low energy excitations in the Luttinger model behave like

*particles* with well-defined energy and momentum. In second quantization, such a particle-hole excitation is obtained by the action of the density operator  $\rho^\dagger(q)$ :

$$\rho^\dagger(q) = \sum_k c_{k+q}^\dagger c_k \quad (2.8)$$

on the ground state. Such a product of fermion operators behaves like a boson operator and it is this insight that leads the way towards the solution of one-dimensional quantum many-body systems.

## 2.5 Solution of the Tomonaga-Luttinger (TL) model: Brief review

The excitations of the Tomonaga-Luttinger model are waves of density of charge, mass or spin and generally move with different/equal speeds. These excitations are essentially bosonic in nature and have a linear dispersion  $\omega_q = v_F |q|$ . Here  $q$  is the wave number for excitations (momentum transfer) and  $v_F$  is the constant velocity at which all excitations propagate. The strictly linear fermion dispersion is justified if we stay in the regime of low energy excitations which correspond to redistribution of electrons (constituent particles) that lie close to the Fermi surface. As a result of the linear dispersion relation the resulting bosons are free and do not interact.

### 2.5.1 The Hamiltonian

Both the Tomonaga model and the Luttinger model are based on linearization of the electron dispersion near Fermi points. However, the prescription for the large momentum cut-off  $k_c$  is different in the two models. Tomonaga model used a finite cut-off on either side of the Fermi points that limited the k-space available for the momentum. While this prescription considers the natural bandwidth of a real system, it is only soluble asymptotically. Luttinger's model on the other hand includes an infinite dispersion,  $-\infty < k < \infty$ , with the

unphysical negative energy states completely filled.

$$H = H_0 + H_2 + H_4 \quad (2.9)$$

$$H_0 = \sum_{k;r=R,L} v_F(\varepsilon_r k - k_F) : c_{r,k}^\dagger c_{r,k} :, \quad (2.10)$$

$$H_2 = \frac{1}{L} \sum_{p,s,s'} [g_{2\parallel}(p)\delta_{s,s'} + g_{2\perp}(p)\delta_{s,-s'}] : \rho_{+,s}(p)\rho_{-,s'}(-p) :, \quad (2.11)$$

$$H_4 = \frac{1}{2L} \sum_{r,p,s,s'} [g_{4\parallel}(p)\delta_{s,s'} + g_{4\perp}(p)\delta_{s,-s'}] : \rho_{r,s}(p)\rho_{r,s'}(-p) :, \quad (2.12)$$

$$(2.13)$$

where  $\varepsilon_r$ ,  $+1$  for right moving electrons and  $-1$  for left moving electrons, characterizes the two infinite branches of the spectrum. To avoid the infinities due to an infinite number of filled states, a normal ordering convention is used which essentially represents fluctuations over the ground state, for example,

$$\rho_{r,s} = \sum_k : c_{r,k+p,s}^\dagger c_{r,k,s} := \sum_k (c_{r,k+p,s}^\dagger c_{r,k,s} - \delta_{q,0} \langle c_{r,k+p,s}^\dagger c_{r,k,s} \rangle_0). \quad (2.14)$$

The coupling constants  $g_2$  and  $g_4$  represent the forward scattering. An exact solution of the Luttinger model is possible only if the dispersion is strictly linear and the backscattering process  $g_1$  is neglected.

### 2.5.2 Bosonization

For simplicity, let us demonstrate bosonization on the Tomonaga-Luttinger (TL) model which has linear excitation spectrum in momentum  $q$ . In this model, the dispersion relation is broken into two separate branches which are straight lines over the interval  $(-\infty, \infty)$  to achieve true independence of the excitation energy  $E(q)$  on the momentum  $q$ . Although, the Tomonaga-Luttinger model is qualitatively different from the original model, Figure 1.5, their low energy physics is similar. The excitation spectrum for this model is shown in

Figure 2.5.

The non-interacting part of the Hamiltonian of the Tomonaga-Luttinger model in terms of fermion creation and annihilation operators can be written as:

$$H_0 = \sum_{k;r=R,L} v_F(\varepsilon_r k - k_F) c_{r,k}^\dagger c_{r,k}. \quad (2.15)$$

Let us forget about the normal ordering for the time being. For right moving excitations, the energy simplifies to  $E_{R,k}(q) = v_F(k+q) - v_F k = v_F q$ . A natural basis for this problem is the density fluctuation basis 2.17 (see details in [11]). The interaction term in the Hamiltonian is quadratic in density operators and thus *quartic* in fermion creation/annihilation operators:

$$H_{int} = \frac{1}{2\Omega} \sum_q V(q) \rho(q) \rho(-q) \quad (2.16)$$

In the density fluctuation basis the Hamiltonian takes a quadratic form and diagonalization becomes a trivial task. The details of derivation of the bosonized form can be found in [11]. We will only state the final form of the Hamiltonian and the commutation relations here:

$$[\rho_r^\dagger(p), \rho_{r'}^\dagger(p')] = -\delta_{r,r'} \delta_{p,p'} \frac{rpL}{2\pi} \quad (2.17)$$

Thus we see that the commutation relation of density operator is similar to that of *bosonic* operators. This allows us to write the boson creation and annihilation operators as linear combinations of density operators as:

$$b_p^\dagger = \sqrt{\frac{2\pi}{L|p|}} \sum_r Y(rp) \rho_r^\dagger(p) \quad (2.18)$$

$$b_p = \sqrt{\frac{2\pi}{L|p|}} \sum_r Y(rp) \rho_r(-p), \quad (2.19)$$

where  $Y(x)$  is the step function. The commutator of the boson operator  $b_{p_0}$  for any momentum  $p_0 > 0$  with the Hamiltonian (2.15) can be found out using the definition of boson

operators above:

$$[b_{p_0}, H] = v_F p_0 b_{p_0}. \quad (2.20)$$

The Hamiltonian that satisfies the relation (2.20) can also be written as:

$$H \approx \sum_{p \neq 0} v_F |p| b_p^\dagger b_p. \quad (2.21)$$

This is a great simplification as the kinetic energy can be expressed as a quadratic form of bosonic operators. Even in the presence of interaction, the bosonization procedure makes the interaction part of the hamiltonian quadratic in boson operators.

Therefore, bosonization essentially reformulates the Hamiltonian and the second quantized operators into a new Hamiltonian,

$$H = \frac{1}{2\pi} \int dx [u\kappa(\pi\Pi(x))^2 + \frac{u}{\kappa}(\nabla\phi(x))^2]. \quad (2.22)$$

The net effect of interactions and the essential low energy physics of the system are contained within two parameters  $\kappa$  and  $u$ ,

$$u\kappa = v_F \left( 1 + \frac{g_4}{2\pi v_F} - \frac{g_2}{2\pi v_F} \right) \quad (2.23)$$

$$u/\kappa = v_F \left( 1 + \frac{g_4}{2\pi v_F} + \frac{g_2}{2\pi v_F} \right) \quad (2.24)$$

*Digression: The continuum field representation*

The most recognizable representation of the Luttinger liquid Hamiltonian is when it's represented in terms of continuum quantum fields. It is convenient to introduce two fields at this point:

$$\phi(x), \theta(x) = \mp(N_R \pm N_L) \frac{\pi x}{L} \mp \frac{i\pi}{L} \sum_{p \neq 0} \frac{1}{p} e^{-\alpha|p|/2 - ipx} (\rho_R^\dagger(p) \pm \rho_L^\dagger(p)) \quad (2.25)$$

This is the main advantage of bosonization. Mathematically rigorous treatment can be found in the Appendix of [11]. The final form of the Hamiltonian in the continuum limit ( $L \rightarrow \infty$ ) is represented as:

$$H = \frac{1}{2\pi} \int dx v_F [(\pi\Pi(x))^2 + (\nabla\phi(x))^2] \quad \text{Tomonaga-Luttinger model,} \quad (2.26)$$

where

$$\Pi(x) = \nabla\theta(x) = \pi[\rho_R(x) - \rho_L(x)]$$

is the current operator in one dimension and

$$\nabla\phi(x) = -\pi[\rho_R(x) + \rho_L(x)].$$

## 2.6 Generalization of one-dimensional interacting particles: The Luttinger liquid conjecture

The successful exact solution of the Tomonaga-Luttinger model is attributed to the linearity of the free electron dispersion. We also saw that density interactions written in bosonized form do not remove the bilinearity of the Hamiltonian. The next obvious question is:

*Which properties of the Tomonaga-Luttinger model survive when the free electron dispersion is no longer linear?*

This question was answered by F.D.M. Haldane in the early 1980s, when he conjectured that the low energy physics of any *gapless* one-dimensional quantum many-particle system, (non-linear electronic dispersion) is robust against renormalization of the parameters  $(\kappa_\nu, \nu_\nu)$ , where  $\nu \in \rho, \sigma$  close to the Fermi surface. Further away from the Fermi points, the non-linearity (curvature) of the dispersion gives rise to finite lifetime effects and a resid-

ual boson-boson interaction which was earlier absent in the strictly linear dispersion. These effects fade away as we move closer to the Fermi surface. Haldane supported his conjecture by a series of case studies on solvable one-dimensional problems in his publications [34, 33]. These scattering processes are discussed in a later section where we discuss the Wigner crystal (4.5.1).

## 2.7 Inadequacy of the Tomonaga-Luttinger model and Luttinger liquid theory

The Luttinger model in its original form, although exactly solvable, cannot account for some of the richest effects observed in real one-dimensional systems [54]. Some of the inadequacies of the Tomonaga-Luttinger model are:

1. As we have discussed, the dispersion relation for the original particles in the Tomonaga-Luttinger model is strictly linear:

$$\varepsilon_p = \pm v_F p,$$

and is composed of two separate branches of right-movers and left-movers. Further, the absence of backscattering ( $q \sim 2k_F$ ) in the Tomonaga-Luttinger model conserves the number of right-movers and left-movers separately. In real systems, however, all particles belong to the same spectrum and can scatter from right(left)-moving states into left(right)-moving ones due to interaction induced scattering.

2. Due to the same reason, the absence of backscattering precludes all the effects that are caused by changing number of right and left movers, e.g., true thermal conductance, electric conductance, etc.
3. The solution consists of non-interacting bosonic excitations which prevents thermalization of the liquid.
4. Particle-hole symmetry which is also an artefact of linearized spectrum of parti-

cles, ( $m \rightarrow \infty$ ), results in a system that is devoid of interesting transport phenomena. Coulomb drag is a direct consequences of particle-hole asymmetry where a direct current flowing through one wire induces a potential difference across another wire placed close to it.

## CHAPTER 3

### BEYOND LUTTINGER LIQUID: CURVED DISPERSION

In this chapter, we will show that a linear dispersion relation, found in a Luttinger liquid and the harmonic Wigner crystal, leads to the failure of perturbation theory even in the presence of arbitrarily weak interaction. We will then introduce a non-linearity in the dispersion relation and demonstrate that this approach gets rid of the pathological divergences that prevent the calculation of transport coefficients.

We are breaking away from the historical terminology in this chapter in favor of clarity, as some of the jargon describing Luttinger liquids has evolved to mean different things based on when a study was conducted since Haldane's breakthrough papers [33]. Haldane coined the term 'Luttinger liquid' as a generalization of the Tomonaga-Luttinger model, to include any gapless one-dimensional quantum system and its behavior at low energy. However, including the effects of interaction between bosonic excitations of these systems is difficult and a lot of initial research in 80s and 90s was based on non-interacting approximation. We will call this 'standard Luttinger liquid approximation' as opposed to the beyond Luttinger liquid paradigm where the effects like interaction and curved dispersion are included.

#### 3.1 Failure of perturbation theory: Decay of linear bosons

We have established that general Luttinger liquid of gapless one-dimensional systems can be very simply represented as:

$$H = \sum_k \omega_k a_k^\dagger a_k \tag{3.1}$$

$$\omega_k = v|k|. \tag{3.2}$$

The solution has bosonic excitations in the form of density waves travelling at speed  $v$ . Equation (3.1), with linear dispersion, is the fixed-point Hamiltonian for any one-dimensional massless system even with a curved bare-fermion dispersion. Although, the Luttinger liquid description (3.1) can be used to exactly calculate the properties like correlation functions and phase diagrams for any generic one-dimensional system, it fails to describe non-equilibrium properties like *lifetime of excitations* and *thermalization* of boson distribution function.

The existence of an exact solution to the Luttinger liquid Hamiltonian suggests that it can serve as the starting point of a perturbative solution to a real *one-dimensional Fermi liquid*. It seems that thermalization and decay of excitation can be achieved by augmenting the Luttinger liquid Hamiltonian with some *irrelevant in renormalization group* sense perturbations [34]. Thus, an infinitesimal non-linearity ( $1/m \neq 0$ ) in dispersion can serve as a weak perturbation. This gives rise to a three-boson interaction with a coupling constant proportional to  $1/m$ . However, a naive approach falls into grave difficulties as is evident from the divergent rate of decay of one phonon decaying into two [80]:

$$\tau_q^{-1} \propto \int dq'_1 dq'_2 [\dots] \delta(q - q'_1 - q'_2) \delta(\omega_q - \omega_{q'_1} - \omega_{q'_2}). \quad (3.3)$$

The scattering rate (3.3) derived using Fermi golden rule represents decay of one phonon with wave number  $q$  into two phonons with wave numbers  $q'_1$  and  $q'_2$ . The two Dirac delta functions ensure energy and momentum conservation before and after the event. For Luttinger liquid excitations with linear dispersion,  $\omega(q) = s|q|$ , when  $q$ ,  $q'_1$  and  $q'_2$  are all moving in the same direction, the energy conserving delta function takes the form  $v^{-1} \delta(q - q'_1 - q'_2)$ . Thus, the linearity of the spectrum leads to divergent and unphysical decay rates on the mass shell ( $1/m \rightarrow 0$ ). This is an unphysical result and points towards failure in the perturbative treatment.

### 3.2 Fermionic description: Dynamic structure factor

We will first see the dynamic structure factor of Tomonaga-Luttinger model and how it reflects properties of TL excitations. Then we will start with a simple free fermion dynamic structure factor with natural quadratic dispersion and thereafter add interactions.

The failure of perturbation theory on *standard Luttinger liquid* in capturing the decay of its Bosonic excitations is a well-known problem [34]. Perturbation theory in this case needs a more careful summation method to get rid of the divergences. However, a more natural way to probe the excitations of a system is to study its dynamical response to external fields. *Dynamic response functions* can be used to investigate the effects of interaction and non-linearity of dispersion (of constituent particles) on the properties of a many-body quantum systems. The spectral function  $A(k, \varepsilon)$  and the *Dynamic Structure Factor*,  $S(q, \omega)$ , are such functions and quantify the linear response of particle density of the many-body system to an external field and characterize the excitations of the system.

The dynamic structure factor is defined as the fourier transform of the density-density correlation for the bare particles (fermions here):

$$S(q, \omega) = \int_{-\infty}^{\infty} dt \int_{-\infty}^{\infty} dx e^{i(\omega t - qx)} \langle \rho(x, t) \rho(0, 0) \rangle, \quad (3.4)$$

where,  $\rho(x, t)$  is the density operator and  $\langle \dots \rangle$  is the ensemble average. the dynamic structure factor probes the fermionic correlations and thus bypasses the problematic divergences in the bosonic description of the Luttinger liquid [21, 16]. At zero temperature,  $S(q, \omega)$  is a measure of the absorption coefficient of external field by the excitations of the quantum liquid, i.e., imaginary part of the susceptibility. We shall focus only on its behavior close to the excitation spectrum of the one-dimensional fermions.

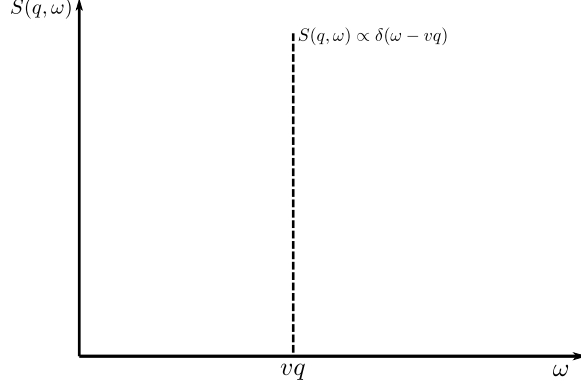


Figure 3.1: Structure factor for Tomonaga-Luttinger model.

### 3.2.1 Linear spinless fermions (Tomonaga-Luttinger model)

The Tomonaga-Luttinger model is the bosonized representation of strictly linear fermion dispersion. Since the relevant physics at low temperatures happens close to the Fermi surface, the quadratic dispersion of free fermions,  $E(k) = k^2/2m$ , can be expanded near the Fermi points as:

$$E(k)_{R/L,k} = \pm v_F(k \pm k_F) + k^2/2m \quad (3.5)$$

$$\xi_{R/L,k} = \pm v_F k + k^2/2m \approx \pm v_F k \quad (3.6)$$

The dynamic structure factor for such fermions is a Dirac delta function (3.2.1) at all temperatures even in the presence of interactions:

$$S_{TL}(q, \omega) \propto q \delta(\omega - vq) \quad \text{Tomonaga-Luttinger.} \quad (3.7)$$

The zero thickness of its peak implies that density waves travelling at a speed  $v$  are the true eigenstates of this system with infinite lifetimes. [11]. Any non-linearity in the dispersion leads to a broadening of the dynamic structure factor even at absolute zero. This leads to rich phenomena even in one-dimensional fermionic systems, for e.g, Coulomb drag is observed experimentally [81, 82, 83] and can be accounted for, theoretically, by considering

a finite width of the structure factor for small wave numbers [21].

### 3.2.2 Free spinless fermions

Let us now consider non-interacting fermions with the quadratic dispersion,

$$\xi(k) = \frac{k^2 - k_F^2}{2m}.$$

Since there is no interaction to induce creation of particle-hole pairs, each particle-hole pair is generated by absorption of an external single photon of momentum ( $\hbar q$ ) and energy ( $\hbar\omega$ ). The energy of such a particle-hole pair lies in the range:

$$\hbar\omega_- < E(q) < \hbar\omega_+, \quad \omega_{\pm} = uq \pm q^2/2m \quad (3.8)$$

defined in equation (3.10). For a given wave number  $q$ , there is a continuous band of possible energies of particle-hole pairs as illustrated in Figure 3.2. The upper edge  $\omega_+$  of this band corresponds to particle at Fermi point jumping to a higher energy state and leaving a hole behind. Similarly, a particle from deep inside the Fermi sea can jump to an empty state just above the Fermi energy. This corresponds to the lower edge of the energy band  $\omega_-$  and leaves behind a hole deep in the Fermi sea. The corresponding dynamic structure factor has a “rectangular peak” of width  $\delta\omega = \omega_+ - \omega_-$  as shown in Figure 3.2. Outside this range of energies, the dynamic structure factor vanishes. The corresponding dynamic structure factor for  $0 < q < 2k_F$  is straightforward to calculate and comes out to be:

$$S_0(q, \omega) = \frac{m}{q} \theta\left(\frac{q^2}{2m} - |\omega - v_F q|\right), \quad (3.9)$$

which can serve as a reference for one-dimensional fermions.  $S_0(q, \omega)$  for free fermions is

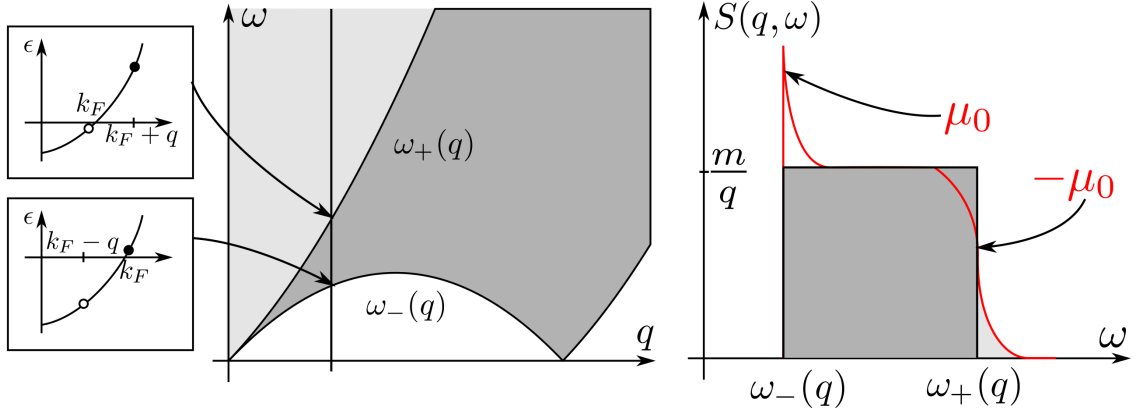


Figure 3.2: (Left) Minimum and maximum energy particle-hole excitations for the same wave number. These excitations form the two edges ( $\omega_{\pm}$ ) of the Structure factor (middle). Structure factor for free particles (shaded rectangle) and development of logarithmic divergence for arbitrarily small interaction between fermions (red).

constant  $m/q$  between  $\omega_-(q)$  and  $\omega_+(q)$  where,

$$\omega_{\pm} = uq \pm q^2/2m, \quad (3.10)$$

branches of excitations and zero elsewhere. We can now *turn-on* a weak interaction and look at the dynamic structure factor of the new *weakly interacting* system.

### 3.2.3 Weakly interacting fermions

Even a small perturbation in interaction modifies the dynamic structure factor of non-interacting fermions in a non-trivial way. The sharp step-like discontinuity of the non-interacting dynamic structure factor at  $\omega = \omega_-$  develops a power-law singularity:

$$\frac{S(q, \omega)}{S_0(q)} = \left( \frac{\delta\omega}{\omega - \omega_-} \right)^{\mu}, \quad 0 < \omega - \omega_- \ll \delta\omega, \quad (3.11)$$

where,  $\delta\omega = \omega_+ - \omega_-$ . However, the dynamic structure factor is still zero for all  $\omega < \omega_-$ . On the right of the peak, the amplitude of the structure factor exhibits decaying leaks into higher energies,  $\omega > \omega_+$ , as depicted in red color in Figure 3.2.

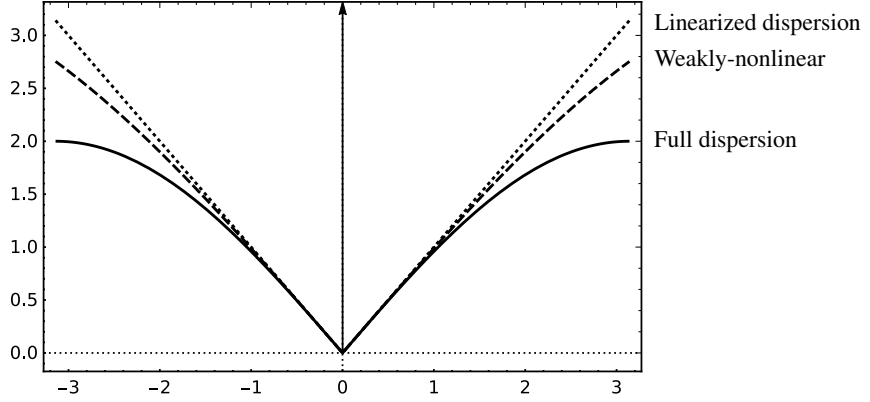


Figure 3.3: Wigner crystal phonons under linear approximation (Luttinger liquid), weak non-linearity  $\xi$ , and exact harmonic dispersion.

*Non-linearity resolves divergences due to interaction*

The bosonic excitations of a Luttinger liquid are exact eigenstates. Further, the concave curvature of the boson excitation dispersion relation does not allow for any decay caused by inter-electron interactions. As a result, these excitations have infinite lifetimes at zero temperature [55, 84]. An alternative approach to resolve this problem is based on the observation that a non-linear dispersion relation can get rid of the divergences in the scattering rates [55]. Consider a weak non-linearity of the form:

$$\omega_q = s|q|(1 - \xi q^2). \quad (3.12)$$

The non-linear part in equation (3.12),  $\xi q^2$ , is justified only in the limit of strong repulsion when the Luttinger parameter  $\kappa = \pi\hbar\rho^2/mv$  is small. Now, if we consider the momentum deep within the classical regime ( $p \gg p^*$ ) [55], we find that each extra phonon in a scattering event contributes a factor of  $\sqrt{K}$  to the scattering amplitude. The dominant contribution will, therefore, come from scattering processes involving as few phonons as possible. For a weak non-linearity, i.e.,  $\xi q^2 \ll 1$ , the decay of a single phonon into two violates energy and momentum conservation. The next best real process is the scattering of two phonons in the initial state into two phonons in the final state. Figure 3.4 shows such a scattering

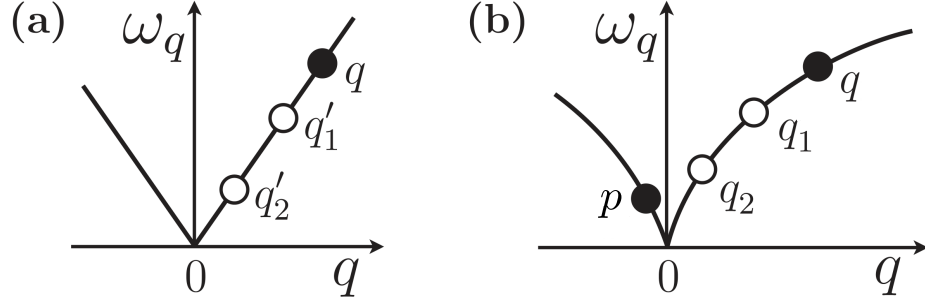


Figure 3.4: (a) Linear dispersion of an ideal Luttinger liquid. The decay of a phonon (filled circle) with wave number  $q$  into two phonons (hollow circles) with wavenumber  $q'_1$  and  $q'_2$  is allowed under energy and momentum conservation but diverges. (b) A non-linearity in the dispersion (3.12) allows a minimum of two phonons each in both initial and final state of a scattering event.

event.

The non-linearity in the dispersion along with energy and momentum conservation dictates that three out of four phonons (two before and two after scattering) should belong to the same branch of the spectrum while the fourth one belongs to the other branch [55]. This can be seen in Figure 3.4b where  $q_2$  belongs to the negative  $q$ -branch and the remaining three phonons  $q_1, q'_1$  and  $q'_2$  lie on the positive  $q$ -branch. The scale of  $q_2$  as compared with other three phonons has the relationship [55]:

$$q_2 \approx -\frac{3}{2}\xi q_1 q'_1 q'_2 \quad (3.13)$$

Equation (3.13) implies that  $q_2$  is of the order of cube root of  $q_1, q'_1$  or  $q'_2$ . This is the dominant scattering process and a parametrically small fraction of the energy of the right moving phonons is thus transferred to the left moving branch (negative  $q$ -branch) resulting in thermalization of energy in the system.

## CHAPTER 4 CALCULATIONS

### 4.1 Wigner crystal

As discussed in section 1.7, a one-dimensional system of interacting particles condenses as a crystal in the limit of strong interaction. For Coulomb interaction, such a configuration is called a Wigner crystal. This happens when the density of electrons follows the following condition 1.8:

$$a_B d^{-2} \ll \rho_0 \ll a_B^{-1} \ln(d/a_B). \quad (4.1)$$

Consider  $N$  identical spinless particles labeled by the dummy index  $l \in [1, N]$  in one-dimension as shown in Figure 4.1. The Hamiltonian of such a system has the form

$$H = \sum_l \frac{p_l^2}{2m} + \frac{1}{2} \sum_{l \neq l'} V(x_l - x_{l'}), \quad (4.2)$$

where  $p_l$  is the linear momentum and  $x_l$  is the position of  $l^{\text{th}}$ . The particles interact via the interaction potential  $V(x)$  while the factor of  $1/2$  takes care of the double counting of pairs of particles. When the particle density is sufficiently low, i.e.,

$$\left. \frac{d^2 V}{dx^2} \right|_{1/\rho} \gg \frac{\hbar^2}{\rho^4 m}, \quad (4.3)$$

the system is in the strongly interacting regime and the particles arrange themselves at a constant distance from each other forming a one-dimensional lattice. In the case when the particles are electrons, such a lattice is called a Wigner crystal [19].

For a classical crystal any finite temperature will cause the particles to oscillate about their mean position. For electrons, the quantum zero-point motion will have the same

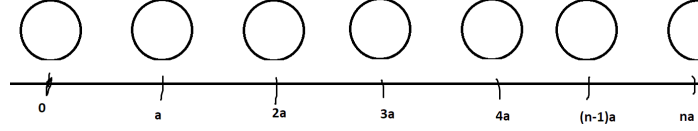


Figure 4.1: Wigner crystal in one-dimension

effect even at absolute temperature. These vibrations wash out the long-range order [19, 38]. The mean distance between two electrons, however, remains close to  $a = 1/\rho$ . Since the amplitude of vibration of a particle is small as compared to the lattice spacing, we can expand the potential  $V(x_l - x_{l'})$  in terms of deviation  $u_l = x_l - l/\rho$  of any particle, from its lattice site as:

$$\begin{aligned} V(x_l - x_{l'}) &= V(al - al' + u_l - u_{l'}) \\ &= V(al - al') + (u_l - u_{l'})V'(al - al') + \frac{1}{2!}(u_l - u_{l'})^2V''(al - al') + \dots \end{aligned}$$

The second term in the above Taylor expansion vanishes because the first derivative of potential is zero at the lattice sites. The first term is a constant energy contribution and can be removed from the Hamiltonian (4.2),

$$H = \sum_{l,l'} \frac{p_l}{2m} + \frac{1}{4}(u_l - u_{l'})^2V''(al - al') + \dots \quad (4.4)$$

The Hamiltonian for the Wigner crystal (4.2) thus takes the following form:

$$H = H_0 + H_3 + H_4 + H_5 \dots, \quad (4.5)$$

where the  $H_0$  is the zeroth order harmonic Hamiltonian:

$$H_0 = \sum_{l,l'} \frac{p_l}{2m} + \frac{1}{4}(u_l - u_{l'})^2V''(al - al') \quad (4.6)$$

The cubic and quartic anharmonic perturbations are

$$H_3 = \sum_{l,l'} \frac{1}{12} (u_l - u_{l'})^3 V^{(3)}(al - al') \quad H_4 = \sum_{l,l'} \frac{1}{48} (u_l - u_{l'})^4 V^{(4)}(al - al'). \quad (4.7)$$

These perturbations give rise to coupling between the non-interacting phonons that form the solution of the zeroth order Hamiltonian  $H_0$ . In the next section we will consider only the  $H_0$  part of the Hamiltonian. This is called the Harmonic approximation.

#### 4.1.1 The Harmonic approximation: Phonons

At low energies the amplitude of oscillation of the particles is very small as compared to the lattice spacing  $1/\rho$ .

$$|u_l - u_{l'}| \ll 1/\rho$$

and the displacement  $u_l - u_{l'}$  from a lattice position indexed by  $l'$  can be expanded in terms of  $l - l'$ . Since the higher order perturbations have increasing powers of displacement, we can ignore the higher orders  $H_3$  and  $H_4$  factors and keep only the leading term in the series,

$$H_0 = \sum_l \frac{p_l^2}{2m} + \frac{1}{2} \sum_{l,l'} V_{l-l'}^{(2)} (u_l - u_{l'})^2. \quad (4.8)$$

Here, we defined the notation

$$V_l^{(m)} = \left. \frac{d^m V(x)}{dx^m} \right|_{x=l/\rho} \quad (4.9)$$

We will now see that  $H_0$ , the *harmonic* term, gives rise to non-interacting phonons. We can write the dynamical variables  $u_l$  and  $p_l$  in terms of second-quantized operators

$$u_l = \sum_q \sqrt{\frac{\hbar}{2mN\omega_q}} (b_q + b_{-q}^\dagger) e^{iql} \quad (4.10)$$

$$p_l = -i \sum_q \sqrt{\frac{\hbar m \omega_q}{2N}} (b_q - b_{-q}^\dagger) e^{iql}. \quad (4.11)$$

The creation operators  $b_q^\dagger$  create a phonon state of momentum  $\hbar q$  and the annihilation operators  $b_q$  destroy a phonon with momentum  $\hbar q$ . These phonon operators satisfy the commutation relation

$$[b_q, b_{q'}^\dagger] = \delta_{q, q'}. \quad (4.12)$$

Since this is the commutation relation satisfied by bosonic operators, it follows that irrespective of whether the particles themselves are bosons or fermions, the excitations of the Wigner crystal (phonons) are always bosonic. The second-quantized Hamiltonian of the harmonic Wigner crystal is thus a quadratic form operator

$$H_0 = \sum_q \hbar \omega_q (b_q^\dagger b_q + 1/2) \quad (4.13)$$

with quantized phonon frequencies

$$\omega_q = \frac{2}{m} \sum_{l=1}^{\infty} V_l^{(2)} [1 - \cos(ql)]. \quad (4.14)$$

The most defining characteristic of these phonons is that they are normal modes and do not couple with each other. The phonons of a harmonic Wigner crystal thus form a gas of non-interacting phonons that travel through the system at finite velocities and do not scatter off each other.

## 4.2 Wigner crystal as Luttinger liquid

Conventional Luttinger liquid theory is the description of a one-dimensional quantum many-body system with gapless bosonic excitations while the excitations of the one-dimensional Wigner crystal are also gapless phonons which are bosonic in nature. This qualitative agreement between the two models begs the question as to how much a Wigner crystal resembles a Luttinger liquid.

It is evident from the non-linear dispersion relation of phonons that they are not truly

identical to the bosonic excitations of a Luttinger liquid. However, if the interaction potential  $V(x)$  between the bare particles falls off faster than  $1/|x|$  at large  $x$  and we restrict the model to low-energy long-wavelength phonons, the dispersion relation becomes linear,

$$\omega_q = v|q|. \quad (4.15)$$

For the purpose of calculational simplicity, we will substitute the group velocity  $v$  with the dimensionless velocity  $s$  such that:

$$s = v\rho. \quad (4.16)$$

These phonons travel at a speed

$$v = \frac{1}{\rho} \sqrt{\frac{V_{22}}{m}}, \quad (4.17)$$

where our notation  $V_{mn}$  is defined as

$$V_{mn} = \sum_{l=1}^{\infty} V_l^{(m)} l^n. \quad (4.18)$$

These excitations and their dispersion relation are identical to the bosonic excitations of a Luttinger liquid which also has linear dispersion. Furthermore, the charge-density correlation calculated using the bosonization method is exactly the same as that of a Wigner crystal [38]. The Wigner crystal under the aforementioned approximations, thus, maps onto the Luttinger liquid with extremely small but positive Luttinger parameter [19],

$$\kappa = \frac{\pi\hbar\rho^2}{ms} \ll 1. \quad (4.19)$$

### 4.3 Ballistic thermal conductance: Harmonic Wigner crystal

A typical setup to measure thermal conductance of a Wigner crystal wire consists of two large thermal reservoirs at equilibrium connected via the wire. Figure 4.2 shows the setup where the temperature of the left reservoir is  $T^+$  and that of the right reservoir is  $(T^-)$ . The



Figure 4.2: Ballistic phonon transport between boson reservoirs.

direction of the net thermal current is from left to right, as is expected from the second law of thermodynamics.

In this section, we will calculate the thermal conductance of the bulk of Wigner crystal quantum wire and disregard the behavior of the leads that connect the wire to the reservoirs. This calculation shows the quantized behavior of thermal conductance. The simplifying assumptions are:

1. *Ideal reservoirs*: the thermal reservoirs are ideal boson reservoirs and their distribution function does not change when they lose heat. In other words, they always remain at the same temperature that they started with and bosonic states inside them always satisfy Bose-Einstein distribution. The thermal conductance just shows energy transmission of non-interacting boson gas.
2. *Reflectionless interfaces*: the interface between the wire and a reservoir is reflectionless, i.e., all phonons that reach the other end of the wire are absorbed into the reservoir without any reflection.
3. *Uniform Wigner crystal*: the lattice spacing is constant for the whole length of the wire. This implies that the Luttinger liquid parameter is independent of position.

The thermal energy of a harmonic Wigner crystal is dominated by the kinetic energy of the excitations of the lattice. A purely harmonic crystal, as discussed in previous chapter, has sound-like excitations with a linear dispersion. In fact, a harmonic one-dimensional Wigner crystal maps onto the ideal Luttinger liquid with free bosonic excitations having

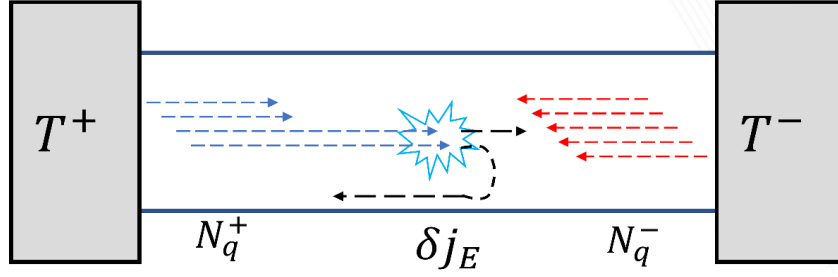


Figure 4.3: A right moving phonon scatters off another right moving phonon. This event leads to a transfer of a small amount of energy to the left moving branch.

a linear dispersion. We will refer to these excitations as bosons or phonons interchangeably. As discussed before, excitations of a harmonic crystal form a non-interacting gas of phonons. These phonons travel from their reservoir of origin across the Wigner crystal wire without scattering off of other phonons. For a clean and isolated Wigner crystal there is no scattering by any impurity or external potential. Thus, this is a case of ballistic transport from one reservoir to the other through the wire. It follows that all the right moving phonons with momentum  $q > 0$  have emanated from the left reservoir ( $T^+$ ) and all the left moving phonons with  $q < 0$  have emanated from the right reservoir ( $T^-$ ). We can conclude that the distribution function ( $N_q^+$ ) of right moving phonons is exactly the same as the equilibrium distribution inside the left reservoir and vice versa. The distribution function inside the wire can be written as:

$$N_q = N_q^+ + N_q^- . \quad (4.20)$$

where,  $N_q^\pm$  is the Bose Einstein distribution function for the phonons originating in left ( $T^+$ ) and right ( $T^-$ ) reservoirs defined as:

$$N_q^\pm = \frac{\theta(\pm q)}{e^{\hbar\omega_q/T^\pm} - 1} . \quad (4.21)$$

The energy current density propagating from left to right  $j_+^0$  and from right to left  $j_-^0$  can

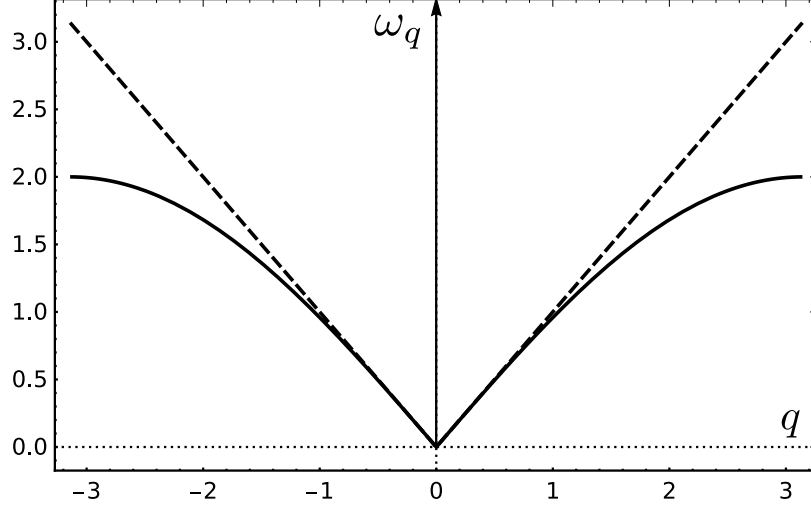


Figure 4.4: Phonon dispersion relation for harmonic Wigner crystal (solid) and linearized low temperature approximation (dashed).

be calculated by summing over individual contribution from each phonon:

$$j_{\pm}^0 = \frac{1}{L} \sum_q \hbar \omega_q \frac{\partial \omega_q}{\partial q} N_q^{\pm} \quad (4.22)$$

where  $\hbar \omega_q$  is the energy associated with a phonon of momentum  $q$ ,  $\partial \omega_q / \partial q$  is the group velocity of a phonon of angular frequency  $\omega_q$  and  $N_q^{\pm}$  is the probability of occupancy of the state with momentum  $\pm q$ .

#### *Low temperature approximation*

At low temperatures, phonons with energy  $\hbar \omega(q) \approx vq \gg k_B T^{\pm}$  have a negligible contribution to the equation (4.22). However, for very long wavelengths, i.e.,  $q \rightarrow 0$  this contribution is still appreciable. Therefore, at low temperatures, equation (4.24) can be approximated as dispersion of phonons upto linear order in  $q$  (at low temperature):

$$\omega(q) = v|q|.$$

*Lattice to continuum*

For a periodic boundary condition, the discrete summation can be converted to an integral under the continuum limit. The phonon wave number, in this limit, is no longer discrete but can take any real positive value:

$$\frac{1}{L} \sum_k \rightarrow \frac{1}{2\pi} \int dk. \quad (4.23)$$

Under these approximations, the thermal current density  $j_{\pm}^0$  takes the form of the integral:

$$j_{\pm}^0 = \frac{1}{2\pi} \int_0^{\infty} \hbar \omega_q \frac{\partial \omega_q}{\partial q} \left( \frac{1}{e^{\hbar \omega_q / T^{\pm}} - 1} \right) dq \quad (4.24)$$

$$= \pm \frac{\hbar v^2}{2\pi} \int_0^{\infty} \frac{q}{e^{\hbar v q / T^{\pm}} - 1} dq. \quad (4.25)$$

Thus, the right propagating and left propagating energy density for spinless bosons comes out to be:

$$j_{\pm}^0 = \pm \frac{\pi T_{\pm}^2}{12\hbar}. \quad (4.26)$$

We can calculate the conductance of this setup as the linear response to a small temperature difference  $\delta T$  between the two reservoirs. The net current due to this small temperature difference, i.e.,  $T^+ - T^- = \delta T$ , can then be calculated using Taylor series expansion of equation (4.3) to linear order in  $\delta T$ , i.e.,

$$j_E = j_+^0 + j_-^0 = \frac{\pi}{6\hbar} T \delta T$$

The thermal conductance of a ballistic Wigner crystal wire is:

$$\boxed{K_0 = \frac{\pi T}{6\hbar}}. \quad (4.27)$$

#### 4.4 Anharmonic perturbations: Interaction between phonons

It is well established [76, 75] that while some properties of crystals are explained in the harmonic limit, it is necessary to consider the anharmonic couplings to model other properties of real crystals. Phenomena such as thermal expansion, thermal conductance, equilibration, etc. need some kind of energy relaxation which can only be provided by scattering and decay of phonons. This requirements makes anharmonic effects indispensable for extending the simple and integrable Luttinger liquid theory to interacting bosonic excitations. Such an extension will help us investigate the violation of the Wiedmann-Franz law.

The leading anharmonic perturbations are the cubic and the quartic terms as defined in equation 4.5 and 4.7. The perturbed Hamiltonian will have the form

$$H \approx H_0 + H_3 + H_4, \quad (4.28)$$

where the anharmonic terms can be expressed in terms of the creation and annihilation operators given in equation 4.10.

$$H_3 = \frac{-i}{3\sqrt{N}} \left( \frac{\hbar}{2m} \right)^{3/2} \sum_{q_1, q_2} \frac{f_3(q_1, q_2)}{\sqrt{\omega_{q_1} \omega_{q_2} \omega_{q_1+q_2}}} (b_{q_1} + b_{-q_1}^\dagger)(b_{q_2} + b_{-q_2}^\dagger) \times (b_{-q_1-q_2} + b_{q_1+q_2}^\dagger) \quad (4.29)$$

$$H_4 = \frac{\hbar^2}{48m^2N} \sum_{q_1, q_2, q_3} \frac{f_4(q_1, q_2, q_3)}{\sqrt{\omega_{q_1} \omega_{q_2} \omega_{q_3} \omega_{q_1+q_2+q_3}}} (b_{q_1} + b_{-q_1}^\dagger)(b_{q_2} + b_{-q_2}^\dagger)(b_{q_3} + b_{-q_3}^\dagger) \times (b_{-q_1-q_2-q_3} + b_{q_1+q_2+q_3}^\dagger). \quad (4.30)$$

The functions  $f_3$  and  $f_4$  are defined as:

$$f_3(q_1, q_2) = \sum_{l=1}^{\infty} V_l^{(3)} \left( \sin\{(q_1 + q_2)l\} - \sin(q_1 l) - \sin(q_2 l) \right) \quad (4.31)$$

$$f_4(q_1, q_2, q_3) = \sum_{l=1}^{\infty} V_l^{(4)} \left( 1 - \cos(q_1 l) - \cos(q_2 l) - \cos(q_3 l) - \cos\{(q_1 + q_2 + q_3)l\} \right. \\ \left. + \cos(\{q_1 + q_2\}l) + \cos(\{q_2 + q_3\}l) + \cos(\{q_3 + q_1\}l) \right). \quad (4.32)$$

## 4.5 Scattering processes in Wigner crystal

The higher order contributions, e.g. the cubic, quartic and so on, can be ignored for a zeroth order calculation. However, violation of the Wiedemann-Franz law calls for the need of improving the approximation beyond the harmonic term. The contribution of higher order terms to the conductance correction gives rise to interaction between the phonons. The mechanism for these corrections in transport properties, e.g., conductance, involve scattering processes between interacting phonons. Thus, calculating these corrections boils down to identifying the dominant scattering processes and calculating their respective contributions.

### 4.5.1 The Umklapp process

One-dimensional Wigner crystal exhibits a rich set of scattering phenomena that show wide variations in the relaxation rates. The slowest of the scattering processes is the *umklapp* scattering which is essentially a scattering that transfers momentum between the phonons and the center-of-mass of the lattice. In an umklapp process the final momentum of the phonon lies outside the first Brillouin zone which maps back into the first Brillouin zone and, thus, the phonon can end up moving in the opposite direction. The change in crystal momentum in an umklapp process has to be close to the reciprocal lattice vector. This means that the energy of the phonon has to be comparable to  $\hbar k_D$ . The statistical distribution of bosons that dictates the mean number of such high energy phonons at low

temperatures,

$$n(k) \approx e^{-\Theta_D/T},$$

decays exponentially as  $T \rightarrow 0$ . Thus, the relaxation time for the umklapp process is large and is a typically slow process compared to other thermalization processes. However, this slowest scattering process makes the leading contribution to the correction to its electrical conductance. This correction is worked out to be [84]:

$$\delta G/G_0 \propto \rho_0 L e^{-\hbar\omega_D/T}, \quad (4.33)$$

where  $G_0 = e^2/h$  is the conductance quantum,  $L$  is the length of the wire and  $\omega_D \sim v\rho_0$  is the Debye frequency.

#### 4.5.2 Non-Umklapp processes

Although the leading correction to  $G$  comes from the umklapp scattering, the corrections in thermal conductance  $K$  is dominated by scattering processes with small momentum transfer. The leading order to these corrections scales as fifth power,  $T^5$ , of the temperature. However, these thermalization processes do not affect the charge transfer and, therefore, are irrelevant in calculation of electrical conductance  $G$ .

### **4.6 Model of our setup: inhomogeneous Luttinger liquid**

We consider a Luttinger liquid connected to two reservoirs. The electron density  $\rho(x)$  varies along the length as a function of position. If the spatial variation of  $\rho(x)$  occurs at a length scale much larger than the fermi wavelength  $\lambda_F$ , the electrons do not suffer backscattering. As a result, the electrical dc conductance is not affected by the inhomogeneity. However, at low temperature, the phonons of the system have wavelengths much longer than the spatial scale of inhomogeneity in the electron density. These inhomogeneities can be treated as a “scattering potential” for the phonons that suffer reflection and transmission

through this potential. If the scattering potential is sharp on the length scale of boundary of the inhomogeneity, the reflection and transmission coefficients show frequency dependent oscillations. The thermal conductance is thus strongly affected by the inhomogeneous electron density. The Hamiltonian in the harmonic approximation of this electron fluid is given by  $H = \int dx \mathcal{H}(x)$  [15], where the Hamiltonian density  $\mathcal{H}$  is:

$$\mathcal{H} = \frac{p^2}{2m\rho(x)} + \frac{1}{2} \left[ V_0 + \frac{\pi^2}{m} \rho(x) \right] (\partial_x \rho u)^2 \quad (4.34)$$

For a constant density Wigner crystal, the low energy Hamiltonian [85] can be expressed as:

$$\mathcal{H} = \frac{p^2}{2m\rho} + \frac{1}{2} m \rho s^2 (\partial_x u(x))^2, \quad (4.35)$$

where,  $s$  is the speed of phonons in the Wigner crystal for given parameters. For the special case of no interaction the phonon speed is same as the Fermi velocity.

#### 4.6.1 Eigenfunctions and eigenvalues

The Hamiltonian (4.34) can be diagonalized by appropriate substitution of dynamical variables. The eigenstates and eigenvalues for periodic boundary conditions over a length  $L$ , for piecewise-constant electron density are:

$$\Phi_\mu = \frac{e^{ik_\mu x}}{\sqrt{L}}, \quad \Omega_\mu = sk_\mu \quad (4.36)$$

The complete wavefunction can, therefore, be obtained by matching the wavefunctions for the three regions in the Wigner crystal at the sharp boundaries. The wavefunction  $\psi_L/\psi_R$  for the phonons originating from left/right reservoir is calculated to be:

$$\psi_L(x, k) = \begin{cases} \frac{1}{\sqrt{L}}(e^{ikx} + r_L(q, k)e^{-ikx}) & x < 0 \\ \frac{1}{\sqrt{L}}((c_L(q, k)e^{iqx} + d_L(q, k)e^{-iqx}) & 0 < x < L_0 \\ \frac{1}{\sqrt{L}}t_L(q, k)e^{ikx} & x > L_0 \end{cases}$$

$$\psi_R(x, k) = \begin{cases} \frac{1}{\sqrt{L}}t_R(q, k)e^{-ikx} & x < 0 \\ \frac{1}{\sqrt{L}}(c_R(q, k)e^{-iqx} + d_R(q, k)e^{iqx}) & 0 < x < L_0 \\ \frac{1}{\sqrt{L}}(e^{-ikx} + r_R(q, k)e^{ikx}) & x > L_0 \end{cases}$$

The wavefunctions  $\psi_L(x, k)$  and  $\psi_R(x, k)$  are orthogonal to each other and themselves,

$$\int \psi_{L/R}(x, k)\psi_{L/R}(x, k'')dx = 0.$$

The coefficients  $c(q, k)$  and  $d(q, k)$  can be solved for by enforcing the continuity and smoothness of wavefunction:

$$c_L(q, k) = -\frac{2k(k+q)}{-(k+q)^2 + (k-q)^2 e^{2iL_0q}} \quad (4.37)$$

$$d_L(q, k) = \frac{2k(k-q)e^{2iL_0q}}{-(k+q)^2 + (k-q)^2 e^{2iL_0q}} \quad (4.38)$$

$$c_R(q, k) = -\frac{2k(k+q)}{-(k+q)^2 + (k-q)^2 e^{-2iL_0q}} \quad (4.39)$$

$$d_R(q, k) = \frac{2k(k-q)e^{2iL_0q}}{-(k+q)^2 + (k-q)^2 e^{-2iL_0q}} \quad (4.40)$$

### *Relation between $q$ and $k$*

We calculated the eigenfunctions, equation 4.6.1, for the whole system of length  $L$ . We can see that for the same energy  $\Omega$ , the wavenumbers in the middle region ( $q$ ) and the ends ( $k$ ) are different. However, the relationship between  $q$  and  $k$  is simple enough and can be found

by taking the ratio,

$$\frac{v}{v_F} \frac{q}{k} = 1$$

$$v_F/v = q/k = \kappa \quad (4.41)$$

If we let  $q/k = \kappa$ , write down equations in terms of  $q$  and  $\kappa$  because we have to treat scattering inside the interacting region of the Luttinger liquid  $\kappa \ll 1$ . We find that the squares of these coefficients are equal for both right moving and left moving phonons, i.e.,  $|c_L|^2 = |c_R|^2 = |c|^2$  and  $|d_L|^2 = |d_R|^2 = |d|^2$ . We will see that we will only need the square of coefficients in our calculations:

$$|c(q, \kappa)|^2 = \frac{2(1 + \kappa)^2}{1 + \kappa^2(6 + \kappa^2) - (\kappa^2 - 1)^2 \cos(2qL_0)} \quad (4.42)$$

$$|d(q, \kappa)|^2 = \frac{2(-1 + \kappa)^2}{1 + \kappa^2(6 + \kappa^2) - (\kappa^2 - 1)^2 \cos(2qL_0)}. \quad (4.43)$$

## 4.7 Correction to thermal conductance

### 4.7.1 Collision integral

The excitations of a harmonic Wigner crystal do not interact with each other and, therefore, have infinite lifetime. Such a gas of phonons never undergoes thermalization. Extending our model to beyond harmonic approximation introduces interaction between phonons. If the interaction potential is weak enough, we can treat the interaction as a perturbation and calculate amplitudes for the phonon-phonon scattering processes. These collisions lead to evolution of the distribution function  $N_q$ . Correction to the thermal conductance of the Wigner crystal can be calculated by keeping track of collisions and the resulting change in

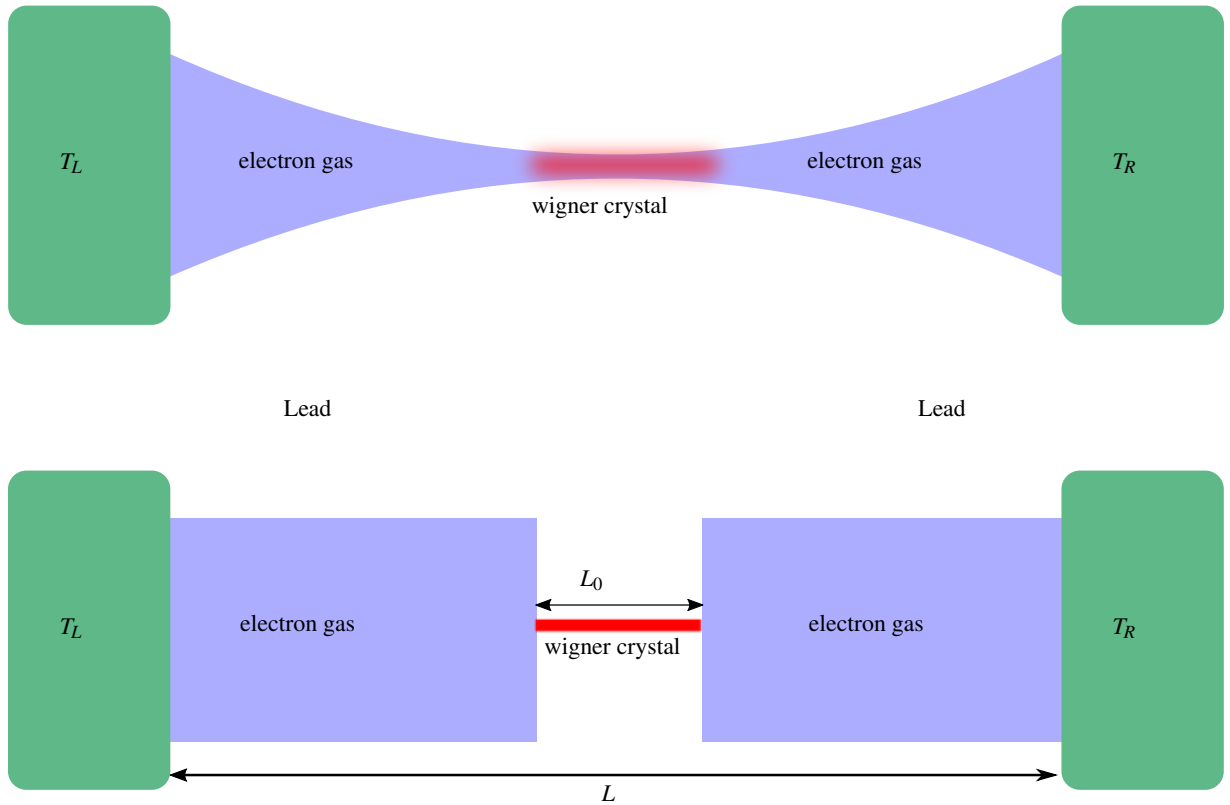


Figure 4.5: (Top) Wigner crystal in a two-dimensional electron gas (2DEG) device forms when the gate voltage is sufficiently high to squeeze the electron channel into a narrow low-density stream. The transition to a Wigner crystal is smooth. (Bottom) Our approximation with a uniform density and a sharp discontinuity between leads and the Wigner crystal. All leads are adiabatically connected to reservoirs ensuring no reflection.

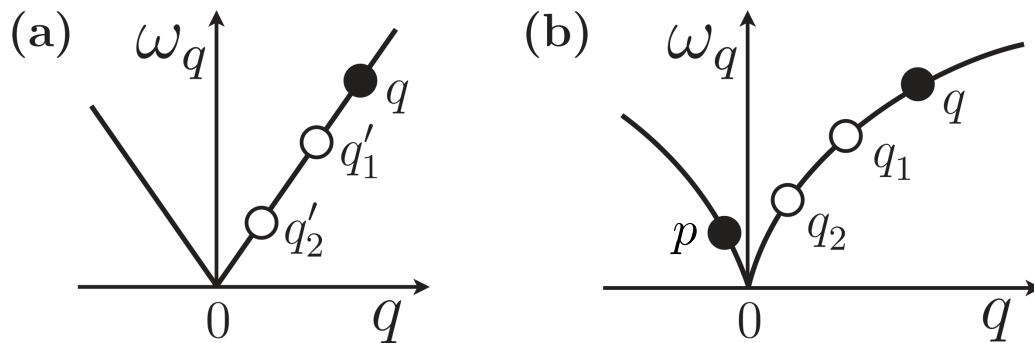


Figure 4.6: (a) A linear dispersion leads to divergences in perturbation theory in interaction for a three phonon process. It also forbids decay of one phonon into two phonons due to violation of energy and momentum conservations. (b) Curvature in the dispersion relation conserves net momentum and energy for a 2 – 2 processes and resolves the mentioned divergence.

flow of thermal current  $j$ . The total current change by an amount  $\delta j$  due to backscattering:

$$j_E = j_+^0 + j_-^0 + \delta j_E, \quad \delta j_E = \frac{d}{dt} E_+, \quad (4.44)$$

where,  $E^+ = \sum_{q>0} \hbar \omega_q N_q$  is the total energy of right moving phonons.

$$\delta j_E = \frac{d}{dt} E_+ = \sum_{q>0} \hbar \omega_q \frac{\partial N_q}{\partial t} \quad (4.45)$$

Using Boltzmann's transport equation for homogenous system and no external field:

$$\frac{\partial N_q}{\partial t} = \mathcal{I}[N_q], \quad (4.46)$$

where,  $\mathcal{I}[N_q]$  is the collision integral which depends on the scattering cross-section and probability of occupation of initial and final states. The collision integral has contributions from the right moving and the left moving phonons:

$$\mathcal{I}[N_q] = \mathcal{I}_{\text{out}}[N_q] + \mathcal{I}_{\text{in}}[N_q]. \quad (4.47)$$

Here,  $\mathcal{I}_{\text{out}}[N_q]$  and  $\mathcal{I}_{\text{in}}[N_q]$  are the contributions for scattering out of state  $q$  and scattering into state  $q$  respectively and can be written as:

$$\mathcal{I}_{\text{out}}[N_q] = - \sum_p \sum_{q_1 > q_2} W_{q,p;q_1,q_2} N_q N_p (1 + N_{q_1})(1 + N_{q_2}) \quad (4.48)$$

$$\mathcal{I}_{\text{in}}[N_q] = + \sum_p \sum_{q_1 > q_2} W_{q,p;q_1,q_2} (1 + N_q)(1 + N_p) N_{q_1} N_{q_2}. \quad (4.49)$$

The scattering rate  $W_{q,p;q_1,q_2}$  is given by [86] :

$$W_{q,p;q_1,q_2} = \frac{2\pi}{\hbar^2} |t_{q,p;q_1,q_2}|^2 \delta_{q+p,q_1+q_2} \quad (4.50)$$

$$\times \delta(\omega_q + \omega_p - \omega_{q_1} - \omega_{q_2}) \quad (4.51)$$

is a function of scattering probability and the Dirac and Kronecker delta functions enforce momentum and energy conservation. Equation 4.46 takes the form:

$$\delta j_E = \sum_{q>0} \hbar \omega_q \sum_{p,q_1,q_2} W_{q,p;q_1,q_2} \mathcal{A}_{q,p;q_1,q_2} \quad (4.52)$$

## 4.8 Approximations and calculation of $\mathcal{A}$ and $W$

Correction to the thermal conductance of the Wigner crystal depends on the higher than harmonic terms of the Hamiltonian and the curvature in the dispersion of the phonons. The dispersion relation for a sufficiently smooth interaction potential is concave.

For a scattering process involving  $n$  phonons, each phonon with wave number  $q$  contributes a factor of  $(\hbar/\omega_q)^{1/2}|q| \propto (\hbar|q|)^{1/2}$  to the scattering amplitude. Therefore, scattering events with a smaller number of phonons will have a higher probability of occurrence. The amplitude for scattering between 3 particles with linear to the dispersion relation diverges. Furthermore, the 3-particle scattering amplitude vanishes as it fails to conserve the total energy and the momentum for a non-linear dispersion. However, allowing the dispersion relation a weak curvature and including a 4<sup>th</sup> phonon with parametrically small momentum as compared to other three phonons results in a non-divergent amplitude while conserving the energy and momentum. The dispersion relation for phonons up to the cubic term is given by:

$$\omega = |q|s(1 - \xi q^2) \quad (4.53)$$

### 4.8.1 Parametrically small momentum transfer

The scattering amplitude can be calculated by using quantum many-body formalism. The non-linearity in the dispersion along with energy and momentum conservation dictates that three out of four phonons (two before and two after scattering) should belong to the same branch of the spectrum while the fourth one belongs to the other branch [55]. This is a characteristic of spectrum non-linearity. Figure 4.6 shows an example of such a process

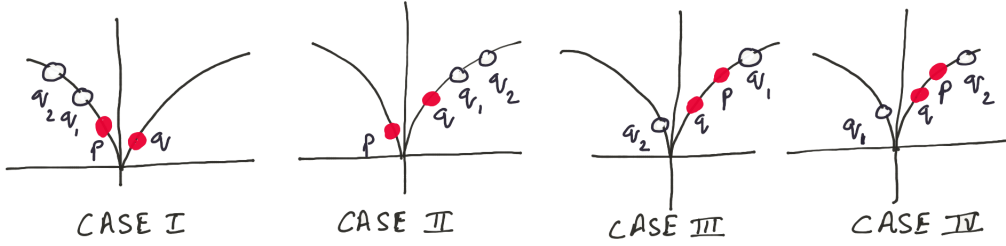


Figure 4.7: Three possible cases of scattering pairs that conserve momentum and energy. These scattering processes contribute to  $\delta j_E$

where  $p$  belongs to the negative  $k$ -branch and the remaining three phonons  $q, q_1$  and  $q_2$  lie on the positive  $k$ -branch. The  $p$  required to fulfill energy conservation for the scattering process has the form [55]:

$$p \approx -\frac{3}{2}\xi qq_1q_2, \quad |p| \ll |q|, |q_1|, |q_2| \quad (4.54)$$

#### 4.8.2 Bose Factors $\mathcal{A}_{q,p;q_1,q_2}$ : Linear response in $\delta T$

The Bose factor is defined as:

$$\mathcal{A}_{q,p;q_1,q_2} = N_q N_p (1 + N_{q_1})(1 + N_{q_2}) - (1 + N_q)(1 + N_p) N_{q_1} N_{q_2}, \quad (4.55)$$

where,  $N(k)$  is the distribution function of the phonon liquid. For a sufficiently short wire, the change in distribution function with distance from the leads can be neglected and  $N(k)$  can be approximated as:

$$N_k \approx N_k^+ + N_k^-. \quad (4.56)$$

$N_k^\pm$  is the Bose distribution function for the phonons originating in left(+,  $L$ ) and right(-,  $R$ ) reservoirs defined as:

$$N_k^\pm = \frac{\theta(\pm k)}{e^{\hbar\omega_k/T^\pm} - 1}. \quad (4.57)$$

Table 4.1: Bose factors for all possible combinations (left column) of reservoirs (Right/Left) of origin of phonons. The phonons have been labeled by their wave numbers  $q, p, q_1, q_2$ .

$q$	$p$	$q_1$	$q_2$	$\mathcal{A}_{q,p,q_1,q_2} T^2 / \hbar \delta T g_q g_p g_{q_1} g_{q_2}$
L	L	L	L	0
R	R	R	R	0
L	L	L	R	$-\omega_{q_2}$
R	R	R	L	$\omega_{q_2}$
L	R	L	L	$\omega_p$
R	L	R	R	$-\omega_p$
L	R	L	R	$\omega_p - \omega_{q_2}$
R	L	R	L	$-\omega_p + \omega_{q_2}$
L	L	R	L	$-\omega_{q_1}$
R	R	L	R	$+\omega_{q_1}$
L	L	R	R	$-\omega_{q_1} - \omega_{q_2}$
R	R	L	L	$\omega_{q_1} + \omega_{q_2}$
L	R	R	L	$\omega_p - \omega_{q_1}$
R	L	L	R	$-\omega_p + \omega_{q_1}$
L	R	R	R	$-\omega_q$
R	L	L	L	$\omega_q$

where,  $T^+(T^-)$  is the temperature of the left (right) reservoir. The thermal conductance is calculated under linear response in the temperature difference

$$\delta T = T^+ - T^-$$

between the two reservoirs.

In each of the scattering cases shown in Figure 4.7, each phonon state can originate from either right (R) or left (L) lead. There are 16 such permutations for each of the 3 scattering cases shown in Figure 4.7, i.e., 48 possible contributions.

The following table lists the approximations to  $\mathcal{A}_{q,p,q_1,q_2}$  in linear response in  $\delta T$  for all 16 reservoir permutations. These have been further simplified using the energy conservation,  $\omega_q + \omega_p = \omega_{q_1} + \omega_{q_2}$ . Here,

$$g_k = [2 \sinh(\hbar \omega_k / T)]^{-1} \quad (4.58)$$

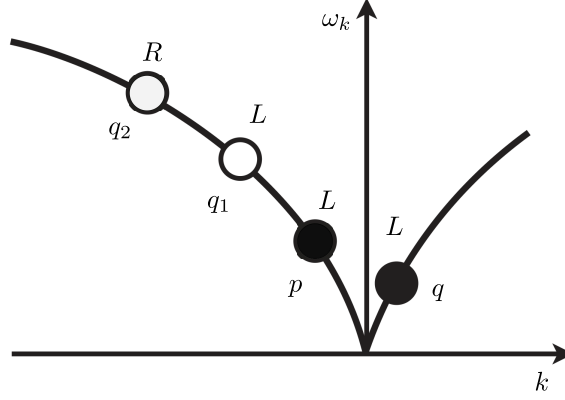


Figure 4.8: An example of a process for case I for inhomogeneous electron density. Phonons  $q, p, q_1, q_2$  originating from L,L,L and R reservoir respectively.

The contributions from LLLL and RRRR should vanish because they represent collisions among particles belonging to an equilibrium Bose-Einstein distribution.

#### *Effect of inhomogeneity of electron density*

The inhomogeneity in the electron density  $\rho(x)$  in the wire is reflected in the Luttinger liquid parameter  $\kappa(x) = \pi\hbar\rho(x)/ms$ . If the wavelength of the phonon is much longer than the length scale related to inhomogeneity of the electron liquid, the change of  $\kappa(x)$  can be approximated to be sharp. The phonons in such a wire have a finite amplitude of reflection from the interface between interacting and non-interacting electron regions. where  $\hat{V}$  is the interaction operator representing cubic and quartic terms of the Wigner crystal,

$$\hat{V} = \hat{H}_3 + \hat{H}_4.$$

Since the interaction potential between two electrons vanishes in the non-interacting region  $x < 0$  and  $x > L$ , only the middle part of the wavefunctions with  $c(k, \kappa)$  and  $d(k, \kappa)$  participates in the scattering amplitude.

From the table of reservoir permutations shown before, we can consider the first non-zero  $\mathcal{A}$  term that belongs to the set LLLR. The amplitude is a sum of 16 terms representing

all  $\pm$  directions for each  $q, p, q_1$  and  $q_2$ .

$$t_{q,p,q_1,q_2} = \int \int dx_1 dx_2 \bar{\psi}_{q_1}^L(x_1) \bar{\psi}_{q_2}^R(x_2) V(x_1 - x_2) \psi_q^L(x_1) \psi_p^L(x_2) \quad (4.59)$$

$$= \int \int dx_1 dx_2 V(x_1 - x_2) \quad (4.60)$$

In the case of inhomogeneous electron density the single particle wavefunctions have the form:

$$\psi_L(x, k) = \frac{1}{\sqrt{L}} \begin{cases} e^{ikx} + r_L(q, k) e^{-ikx} & x < 0 \\ c_L(q, k) e^{iqx} + d_L(q, k) e^{-iqx} & 0 < x < L \\ t_L(q, k) e^{ikx} & x > L \end{cases}$$

There are a total of 256 terms ( $16 \times 16$ ) in the expression for  $\delta K$ , but due to the fact that we are looking at only  $q > 0$  subspace and the energy and momentum conservation, each reservoir combination, e.g. LLLR, has only three allowed cases (e.g. Case I  $\rightarrow q > 0, \{p, q_1, q_2\} < 0$ ) discussed above. Thus a straightforward way will be to start with Case-I (from I,II and III) and combine it with Bose factors  $\mathcal{A}_{q,p,q_1,q_2}$  for all 16 reservoir combinations.

$$\mathcal{A}_{q,p,q_1,q_2}^{LLLL}$$

The contribution to  $\delta K$  for reservoir combination LLLR, i.e.  $\mathcal{A}_{q,p,q_1,q_2}^{LLLL}$ . To understand the calculation of the scattering amplitude and Bose factor  $\mathcal{A}_{q,p,q_1,q_2}^{LLLL}$ , consider the two body interaction operator  $\hat{V}_{q,p,q_1,q_2}^{LLLL}$  for the LLLR permutation,

$$\hat{V}_{q,p,q_1,q_2}^{LLLL} = \sum_{q,p,q_1,q_2} a_{q_1}^\dagger a_{q_2}^\dagger a_q a_p \int \int dx_1 dx_2 \bar{\psi}_{q_1}^L(x_1) \bar{\psi}_{q_2}^R(x_2) V(x_1 - x_2) \psi_q^L(x_1) \psi_p^L(x_2) \quad (4.61)$$

Let  $x_1 - x_2 = y$  and  $x_2 = x$ ,

$$\begin{aligned}
\hat{V}_{q,p;q_1,q_2}^{LLL} &= \sum_{q,p,q_1,q_2} a_{q_1}^\dagger a_{q_2}^\dagger a_q a_p \int \int dx dy (c_{q_2}^* e^{iq_2 x}) (d_{q_1}^* e^{iq_1(x+y)}) V(y) (c_q e^{iq(x+y)}) (d_p e^{-ipx}) \\
&= \sum_{q,p,q_1,q_2} a_{q_1}^\dagger a_{q_2}^\dagger a_q a_p c_{q_2}^* d_{q_1}^* c_q d_p \int dx e^{ix(q_1+q_2+q-p)x} \int dy V(y) e^{i(q+q_1)y} \\
\hat{V}_{q,p;q_1,q_2}^{LLL} &= \sum_{q,p,q_1,q_2} a_{q_1}^\dagger a_{q_2}^\dagger a_q a_p c_{q_2}^* d_{q_1}^* c_q d_p \delta(q_1 + q_2 + q - p) \tilde{V}(q + q_1)
\end{aligned}$$

Following the same treatment, we can calculate the full operator  $\hat{V}_{q,p;q_1,q_2}^{LLLL}$ :

$$\hat{V}_{q,p;q_1,q_2}^{LLLL} = \sum_{q,p,q_1,q_2} a_{q_1}^\dagger a_{q_2}^\dagger V_{q,p;q_1,q_2}^{LLLL} a_p a_q \quad (4.62)$$

$$\text{where } V_{q,p;q_1,q_2} = V(q+q_1) c_p^L d_q^L \delta(p-q-q_1-q_2) \bar{c}_{q_1}^L \bar{d}_{q_2}^R + \\ V(q-q_1) c_p^L d_q^L \delta(p-q+q_1-q_2) \bar{d}_{q_1}^L \bar{d}_{q_2}^R + \quad (4.63)$$

$$V(q+q_1) c_q^L d_p^L \delta(-p+q+q_1-q_2) \bar{d}_{q_1}^L \bar{d}_{q_2}^R + \quad (4.64)$$

$$V(q+q_1) c_p^L d_q^L \delta(p-q-q_1+q_2) \bar{c}_{q_1}^L \bar{c}_{q_2}^R + \quad (4.65)$$

$$V(q-q_1) c_q^L d_p^L \delta(-p+q-q_1+q_2) \bar{c}_{q_1}^L \bar{c}_{q_2}^R + \quad (4.66)$$

$$V(q-q_1) c_p^L d_q^L \delta(p-q+q_1+q_2) \bar{c}_{q_2}^R \bar{d}_{q_1}^L + \quad (4.67)$$

$$\rightarrow V(q-q_1) c_q^L d_p^L \delta(p-q+q_1+q_2) \bar{c}_{q_1}^L \bar{d}_{q_2}^R + \quad (4.68)$$

$$\rightarrow V(q+q_1) c_q^L d_p^L \delta(-p+q+q_1+q_2) \bar{c}_{q_2}^R \bar{d}_{q_1}^L + \quad (4.69)$$

$$V(q-q_1) c_p^L c_q^L \delta(p+q-q_1-q_2) \bar{c}_{q_1}^L \bar{d}_{q_2}^R + \quad (4.70)$$

$$\rightarrow V(q+q_1) c_p^L c_q^L \delta(p+q+q_1-q_2) \bar{d}_{q_1}^L \bar{d}_{q_2}^R + \quad (4.71)$$

$$V(q+q_1) c_p^L c_q^L \delta(p+q+q_1+q_2) \bar{c}_{q_2}^R \bar{d}_{q_1}^L + \quad (4.72)$$

$$\rightarrow V(q-q_1) c_p^L c_q^L \delta(p+q-q_1+q_2) \bar{c}_{q_1}^L \bar{c}_{q_2}^R + \quad (4.73)$$

$$V(q+q_1) d_p^L d_q^L \delta(p+q+q_1-q_2) \bar{c}_{q_1}^L \bar{c}_{q_2}^R + \quad (4.74)$$

$$V(q-q_1) d_p^L d_q^L \delta(-p-q+q_1+q_2) \bar{c}_{q_2}^R \bar{d}_{q_1}^L + \quad (4.75)$$

$$V(q+q_1) d_p^L d_q^L \delta(p+q+q_1+q_2) \bar{c}_{q_1}^L \bar{d}_{q_2}^R + \quad (4.76)$$

$$V(q-q_1) d_p^L d_q^L \delta(p+q-q_1+q_2) \bar{d}_{q_1}^L \bar{d}_{q_2}^R, \quad (4.77)$$

where  $a_k$  and  $a_k^\dagger$  are the annihilation and creation operators. It is important to know that the values of  $q, p, q_1, q_2$  are all positive. We will transform the final answer in a more intuitive/physical form at the end of this calculation. The energy and momentum conservation

implies that only four of the above terms are allowed:

$$V_{q,p;q_1,q_2}^{LLLR} = V(q - q_1) c^L_q d^L_p \delta(q - p - q_1 - q_2) \bar{c}^L_{q_1} \bar{d}^R_{q_2} + \quad (4.78)$$

$$V(q + q_1) c^L_q d^L_p \delta(q - p + q_1 + q_2) \bar{c}^R_{q_2} \bar{d}^L_{q_1} + \quad (4.79)$$

$$V(q + q_1) c^L_p c^L_q \delta(q + p + q_1 - q_2) \bar{d}^L_{q_1} \bar{d}^R_{q_2} + \quad (4.80)$$

$$V(q - q_1) c^L_p c^L_q \delta(q + p - q_1 + q_2) \bar{c}^L_{q_1} \bar{c}^R_{q_2}. \quad (4.81)$$

We can make appropriate substitutions which transform all delta functions to the form  $\delta(q + p - q_1 - q_2)$  and all  $V(q \pm q_1)$  into  $V(q - q_1)$ . For example:  $V_{q,p;q_1,q_2}^{LLLR}$  above will transform into:

$$\begin{aligned} V_{q,p;q_1,q_2}^{LLLR} = & \left[ c^L_q d^L_p \bar{c}^L_{q_1} \bar{d}^R_{q_2} \quad q > 0, p < 0, q_1 > 0, q_2 > 0 \quad \text{Case - II} \right. \\ & + c^L_q d^L_p \bar{c}^R_{q_2} \bar{d}^L_{q_1} \quad q > 0, p < 0, q_1 < 0, q_2 < 0 \quad \text{Case - I} \\ & + c^L_p c^L_q \bar{d}^L_{q_1} \bar{d}^R_{q_2} \quad q > 0, p > 0, q_1 < 0, q_2 > 0 \quad \text{Case - IV} \\ & \left. + c^L_p c^L_q \bar{c}^L_{q_1} \bar{c}^R_{q_2} \quad q > 0, p > 0, q_1 > 0, q_2 < 0 \quad \text{Case - III} \right] \\ & \times V(q - q_1) \delta(q + p - q_1 - q_2) \end{aligned} \quad (4.82)$$

The coefficients of the bose factors on the basis of the source of phonons (reservoirs) and the direction of propagation are summarized in Table 4.8.2. The  $c$  and  $d$  factors come into play because of multiple reflections between the two sharp interfaces of interacting and non-interacting electrons liquid.

### 4.8.3 Scattering probability $W_{q,p;q_1,q_2}$

The phonon number conserving scattering amplitude between two phonons shown in Figure 4.7 describe the simplest possible *real* scattering process. The amplitude of such processes has contributions from the first order in quartic anharmonicity and second order in cubic anharmonicity of the Hamiltonian. Each real phonon contributes a factor of

Table 4.2: Table showing calculated  $c$  and  $d$  factors to be used in the integrals for correction to thermal conductance.

$q$	$p$	$q_1$	$q_2$	CASE-I	CASE-II	CASE-III	CASE-IV	$\mathcal{A}$
L	L	L	R	$c_q d_p d_{q_1}^* c_{q_2}^*$	$c_q d_p c_{q_1}^* d_{q_2}^*$	$c_q c_p c_{q_1}^* c_{q_2}^*$	$c_q c_p d_{q_1}^* d_{q_2}^*$	$-\omega_{q_2}$
R	R	R	L	$d_q c_p c_{q_1}^* d_{q_2}^*$	$d_q c_p d_{q_1}^* c_{q_2}^*$	$d_q d_p d_{q_1}^* d_{q_2}^*$	$d_q d_p c_{q_1}^* c_{q_2}^*$	$\omega_{q_2}$
L	R	L	L	$c_q c_p d_{q_1}^* d_{q_2}^*$	$c_q c_p c_{q_1}^* c_{q_2}^*$	$c_q d_p c_{q_1}^* d_{q_2}^*$	$c_q d_p d_{q_1}^* c_{q_2}^*$	$\omega_p$
R	L	R	R	$d_q d_p c_{q_1}^* c_{q_2}^*$	$d_q d_p d_{q_1}^* d_{q_2}^*$	$d_q c_p d_{q_1}^* c_{q_2}^*$	$d_q c_p c_{q_1}^* d_{q_2}^*$	$-\omega_p$
L	R	L	R	$c_q c_p d_{q_1}^* c_{q_2}^*$	$c_q c_p c_{q_1}^* d_{q_2}^*$	$c_q d_p c_{q_1}^* c_{q_2}^*$	$c_q d_p d_{q_1}^* d_{q_2}^*$	$\omega_p - \omega_{q_2}$
R	L	R	L	$d_q d_p c_{q_1}^* d_{q_2}^*$	$d_q d_p d_{q_1}^* c_{q_2}^*$	$d_q c_p d_{q_1}^* d_{q_2}^*$	$d_q c_p c_{q_1}^* c_{q_2}^*$	$-\omega_p + \omega_{q_2}$
L	L	R	L	$c_q d_p c_{q_1}^* d_{q_2}^*$	$c_q d_p d_{q_1}^* c_{q_2}^*$	$c_q c_p d_{q_1}^* d_{q_2}^*$	$c_q c_p c_{q_1}^* c_{q_2}^*$	$-\omega_{q_1}$
R	R	L	R	$d_q c_p d_{q_1}^* c_{q_2}^*$	$d_q c_p c_{q_1}^* d_{q_2}^*$	$d_q d_p c_{q_1}^* c_{q_2}^*$	$d_q d_p d_{q_1}^* d_{q_2}^*$	$\omega_{q_1}$
L	L	R	R	$c_q d_p c_{q_1}^* c_{q_2}^*$	$c_q d_p d_{q_1}^* d_{q_2}^*$	$c_q c_p d_{q_1}^* c_{q_2}^*$	$c_q c_p c_{q_1}^* d_{q_2}^*$	$-\omega_{q_1} - \omega_{q_2}$
R	R	L	L	$d_q c_p d_{q_1}^* d_{q_2}^*$	$d_q c_p c_{q_1}^* c_{q_2}^*$	$d_q d_p c_{q_1}^* d_{q_2}^*$	$d_q d_p d_{q_1}^* c_{q_2}^*$	$\omega_{q_1} + \omega_{q_2}$
L	R	R	L	$c_q c_p c_{q_1}^* d_{q_2}^*$	$c_q c_p d_{q_1}^* c_{q_2}^*$	$c_q d_p d_{q_1}^* d_{q_2}^*$	$c_q d_p c_{q_1}^* c_{q_2}^*$	$\omega_p - \omega_{q_1}$
R	L	L	R	$d_q d_p d_{q_1}^* c_{q_2}^*$	$d_q d_p c_{q_1}^* d_{q_2}^*$	$d_q c_p c_{q_1}^* c_{q_2}^*$	$d_q c_p d_{q_1}^* d_{q_2}^*$	$-\omega_p + \omega_{q_1}$
L	R	R	R	$c_q c_p c_{q_1}^* c_{q_2}^*$	$c_q c_p d_{q_1}^* d_{q_2}^*$	$c_q d_p d_{q_1}^* c_{q_2}^*$	$c_q d_p c_{q_1}^* d_{q_2}^*$	$-\omega_q$
R	L	L	L	$d_q d_p d_{q_1}^* d_{q_2}^*$	$d_q d_p c_{q_1}^* c_{q_2}^*$	$d_q c_p c_{q_1}^* d_{q_2}^*$	$d_q c_p d_{q_1}^* c_{q_2}^*$	$\omega_q$

$(\hbar/\omega_q)^{1/2}|q| = (\hbar|q|)^{1/2}$  which makes a four phonon scattering amplitude proportional to  $\hbar^2$ .

### Amplitude of scattering

The transition matrix for the scattering process is:

$$t_{q,p \rightarrow q_1, q_2} = \frac{\hbar^2}{m^3 N} \frac{\Lambda}{(\omega_q \omega_p \omega_{q_1} \omega_{q_2})^{1/2}}, \quad (4.83)$$

where  $\Lambda$  is calculated to be

$$\Lambda = -\frac{f_3(q_1, q_2) f_3(q, p)}{\omega_{q_1+q_2}^2 - (\omega_{q_1} + \omega_{q_2})^2} + \frac{f_3(q_2, -q) f_3(q_1, -p)}{\omega_{q_2-q}^2 - (\omega_{q_2} - \omega_q)^2} + \frac{f_3(q_1, -q) f_3(q_2, -p)}{\omega_{q_2-p}^2 - (\omega_{q_2} - \omega_p)^2} + \frac{m}{2} f_4(q_1, q_2, -q) \quad (4.84)$$

The amplitude for small  $q, p, q_1, q_2$  is calculated in [84]:

$$t_{q,p;q_1,q_2} = \frac{\lambda \hbar^2 \rho^2}{N m} |qpq_1q_2|^{1/2}. \quad (4.85)$$

*Calculation of  $\delta j_E$*

We can now setup the Boltzmann kinetic equation in solvable form by using the scattering amplitudes and Bose factors derived above.

$$\delta j_E = \sum_{q>0} \hbar \omega_q \sum_{p,q_1,q_2} W_{q,p;q_1,q_2} \mathcal{A}_{q,p;q_1,q_2} \quad (4.86)$$

For the lead combination *LLLR*, the equation can be written with  $W_{q,p;q_1,q_2}^{LLLR}$  and  $\mathcal{A}_{q,p;q_1,q_2}^{LLLR}$ . It should be noted that the scattering amplitude  $W_{q,p;q_1,q_2}$  for a uniform Luttinger liquid is only dependent on the wavefunctions of phonons and the inter-phonon interaction potential. Our scattering probability contains the factors  $c(q,L)$  and  $d(q,L)$  because of the reflections at the sharp interface of the inter-phonon interaction that drops to zero outside the interacting region. Let us call the no-reflection scattering probability  $W_{q,p;q_1,q_2}^{homogenous}$  defined as:

$$W_{q,p;q_1,q_2}^{LLLR} = W_{q,p;q_1,q_2}^{homogenous} (c_q d_p d_{q_1}^* c_{q_2}^* + c_q d_p c_{q_1}^* d_{q_2}^* + c_q c_p c_{q_1}^* c_{q_2}^* + c_q c_p d_{q_1}^* d_{q_2}^*) \quad (4.87)$$

$$\begin{aligned} \delta j_E^{LLLR} &= \sum_{q^+} \hbar \omega_q \sum_{pq_1q_2} W_{q,p;q_1,q_2}^{LLLR} \mathcal{A}_{q,p;q_1,q_2}^{LLLR} \\ &= \sum_{q^+} \hbar \omega_q \left[ \sum_{p^+q_1^+q_2^+} W_{q,p;q_1,q_2}^{homogenous} |c_q d_p d_{q_1}^* c_{q_2}^*|^2 + \sum_{p^+q_1^+q_2^+} W_{q,p;q_1,q_2}^{homogenous} |c_q d_p c_{q_1}^* d_{q_2}^*|^2 + \right. \\ &\quad \left. \sum_{p^+q_1^+q_2^+} W_{q,p;q_1,q_2}^{homogenous} |c_q c_p c_{q_1}^* c_{q_2}^*|^2 + \sum_{p^+q_1^+q_2^+} W_{q,p;q_1,q_2}^{homogenous} |c_q c_p d_{q_1}^* d_{q_2}^*|^2 \right] \mathcal{A}_{q,p;q_1,q_2}^{LLLR} \end{aligned} \quad (4.88)$$

#### 4.9 Artifacts of our model and how to eliminate them

The expression derived above (4.93) contains squares of complex factors  $c_q$  and  $d_q$ :

$$|c(q, \kappa)|^2 = \frac{2(1 + \kappa)^2}{1 + \kappa^2(6 + \kappa^2) - (\kappa^2 - 1)^2 \cos(2qL_0)} \quad (4.89)$$

$$|d(q, \kappa)|^2 = \frac{2(-1 + \kappa)^2}{1 + \kappa^2(6 + \kappa^2) - (\kappa^2 - 1)^2 \cos(2qL_0)}. \quad (4.90)$$

The oscillation term,  $\cos(2qL_0)$  in these factors lead to oscillations about a mean in the final expression,  $\delta j_E$ , for the change of energy current. These oscillations are a result of unnatural and sharp change in the interaction potential at the interface of interacting and non-interacting electron liquid. Since the potential decays smoothly over a certain length scale, we want the long length limit of the quantum wire  $L \rightarrow \infty$ . To remove the oscillations we need to find the average of this function. This can be done fairly easily at this point in our calculation. Carrying these oscillations to the end and then taking the mean will also give the same result. We will use the fact that mean of the product of mutually independent functions is equal to the product of their means:

$$\overline{f(x)g(y)h(z)} = \overline{f(x)} \overline{g(y)} \overline{h(z)}$$

*Mean of  $|c_q|^2$  and  $|d_q|^2$*

Equations (4.89) can be integrated with respect to the argument of the cosine term:

$$\text{mean}(|c|^2) = \frac{1}{2\pi} \int_0^{2\pi} dx \frac{2(1 + \kappa)^2}{1 + \kappa^2(6 + \kappa^2) - (\kappa^2 - 1)^2 \cos(x)} = \frac{(\kappa + 1)^2}{2(\kappa^3 + \kappa)} \quad (4.91)$$

$$\text{mean}(|d|^2) = \frac{1}{2\pi} \int_0^{2\pi} dx \frac{2(\kappa - 1)^2}{1 + \kappa^2(6 + \kappa^2) - (\kappa^2 - 1)^2 \cos(x)} = \frac{(\kappa - 1)^2}{2(\kappa^3 + \kappa)}. \quad (4.92)$$

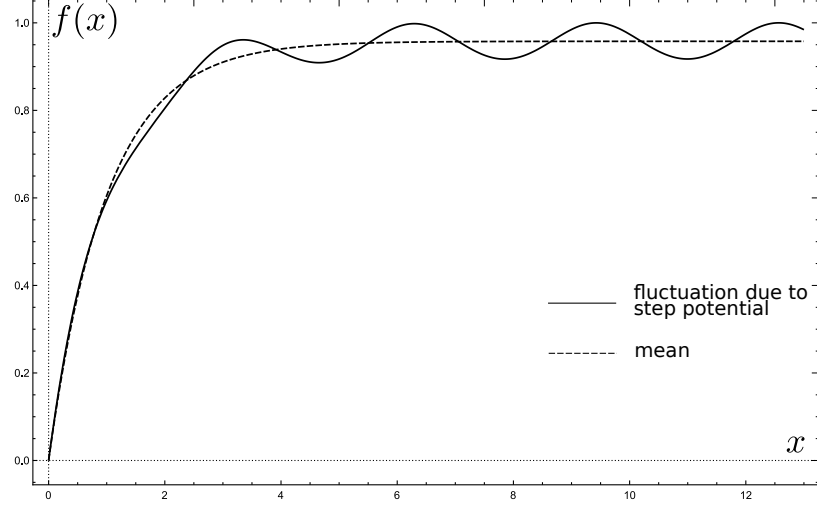


Figure 4.9: [Averaging over the oscillations of a function.]An illustrative figure showing how our *averaging* eliminates the oscillations (solid line) due to sharp potential step. We desire the mean behavior (dotted) of this function.

The means  $(|c|^2)$  and  $(|d|^2)$  are independent of the wave numbers  $q, p, q_1, q_2$ . This brings the change in energy current to the following form:

$$\begin{aligned}
\delta j_E^{LLL} &= \sum_{q^+} \hbar \omega_q \sum_{pq_1q_2} W_{q,p;q_1,q_2}^{LLL} \mathcal{A}_{q,p;q_1,q_2}^{LLL} \\
&= \sum_{q^+} \hbar \omega_q \left[ \sum_{p^-q_1^+q_2^+} W_{q,p;q_1,q_2}^{homogenous} |cddc|^2 + \sum_{p^-q_1^-q_2^-} W_{q,p;q_1,q_2}^{homogenous} |cdcd|^2 + \right. \\
&\quad \left. \sum_{p^+q_1^+q_2^-} W_{q,p;q_1,q_2}^{homogenous} |cccc|^2 + \sum_{p^+q_1^-q_2^+} W_{q,p;q_1,q_2}^{homogenous} |ccdd|^2 \right] \mathcal{A}_{q,p;q_1,q_2}^{LLL} \quad (4.93)
\end{aligned}$$

Similarly, we can derive the expressions for  $\delta j_E^{LLL}, \delta j_E^{RRR}, \delta j_E^{LRL}, \dots, \delta j_E^{RLL}$ . Grouping together the summations on same subspace, e.g.  $\{q^+ p^- q_1^- q_2^-\}$ , we can calculate the change

in energy current due to each of the four scattering processes:

$$\begin{aligned} \delta j_E^I = & \sum_{q^+ p^- q_1^- q_2^-} \hbar \omega_q W_{q,p;q_1,q_2}^{homogenous} \left[ -\omega_{q_2} |cddc|^2 + \omega_{q_2} |dccd|^2 + \omega_p |ccdd|^2 - \right. \\ & \omega_p |ddcc|^2 + (\omega_p - \omega_{q_2}) |ccdc|^2 + (-\omega_p + \omega_{q_2}) |ddcd|^2 - \omega_{q_1} |cdcd|^2 \\ & + \omega_{q_1} |dcdc|^2 - (\omega_{q_1} + \omega_{q_2}) |cdcc|^2 + (\omega_{q_1} + \omega_{q_2}) |dcdd|^2 + \\ & \left. (\omega_p - \omega_{q_1}) |cccd|^2 + (-\omega_p + \omega_{q_1}) |dddc|^2 - \omega_q |cccc|^2 + \omega_q |dddd|^2 \right] \frac{\hbar \delta T}{T^2} g_q g_p g_{q_1} g_{q_2} \end{aligned}$$

Under the energy conservation constraint, the term above in square brackets simplifies to:

$$-(c-d)(c+d)^3 \omega_q = -\frac{4\omega_q}{\kappa(1+\kappa^2)^2}. \quad (4.94)$$

Similar calculations for all four contributions can be calculated. The simplified expressions for the these contributions are

$$\delta j_E^I = (d-c)(c+d)^3 \sum_{q^+ p^- q_1^- q_2^-} (\hbar \omega_q)^2 W_{q,p;q_1,q_2}^{homogenous} \frac{\delta T}{T^2} g_q g_p g_{q_1} g_{q_2} \quad (4.95)$$

$$\delta j_E^{II} = (c-d)(c+d)^3 \sum_{q^+ p^- q_1^+ q_2^+} (\hbar \omega_q)(\hbar \omega_p) W_{q,p;q_1,q_2}^{homogenous} \frac{\delta T}{T^2} g_q g_p g_{q_1} g_{q_2} \quad (4.96)$$

$$\delta j_E^{III} = (d-c)(c+d)^3 \sum_{q^+ p^+ q_1^+ q_2^-} (\hbar \omega_q)(\hbar \omega_{q_2}) W_{q,p;q_1,q_2}^{homogenous} \frac{\delta T}{T^2} g_q g_p g_{q_1} g_{q_2} \quad (4.97)$$

$$\delta j_E^{IV} = (d-c)(c+d)^3 \sum_{q^+ p^+ q_1^- q_2^+} (\hbar \omega_q)(\hbar \omega_{q_1}) W_{q,p;q_1,q_2}^{homogenous} \frac{\delta T}{T^2} g_q g_p g_{q_1} g_{q_2}. \quad (4.98)$$

### *Leading order of integrals*

The above  $\delta j$  contributions will be very difficult to evaluate. Fortunately, we only need the leading order in temperature for these terms.  $\delta j_E^{III}$  and  $\delta j_E^{IV}$  should be equal because Case III and Case IV are essentially the same scattering processes due to indistinguishability of phonons. It is useful to notice that there are three phonons on one branch and one

phonon on the opposite branch of phonons. The single phonon on the opposite branch has a parametrically smaller momentum than the other three. For example, in  $\delta j_E^I$ ,  $|q| \ll |p|, |q_1|, |q_2|$ , we can expand the leading term of the factor

$$\frac{\hbar\omega_q}{T} g_q = \frac{\hbar\omega_q}{T} \left[ 2 \sinh \left( \frac{\hbar\omega_q}{2T} \right) \right]^{-1} \approx 1 \quad (4.99)$$

The Kronecker delta function and the Dirac delta can be approximated as:

$$\delta_{q+p, q_1+q_2} \approx \delta_{p, q_1+q_2}, \quad (4.100)$$

$$\delta(q+p-q_1-q_2) \approx \frac{1}{2s} \delta\left(q + \frac{3}{2} \xi q_1 q_2 p\right), \quad (4.101)$$

which brings  $\delta j_E^I$  to the following form:

$$\delta j_E^I = (d-c)(c+d)^3 \frac{\delta T}{T} \sum_{q^+ p^- q_1^- q_2^-} \hbar\omega_q \left[ \frac{2\pi}{\hbar^2} |t_{q,p;q_1,q_2}|^2 \right] \frac{1}{2s} \delta\left(q + \frac{3}{2} \xi q_1 q_2 p\right) \delta_{p, q_1+q_2} g_p g_{q_1} g_{q_2}. \quad (4.102)$$

We can substitute  $t_{q,p;q_1,q_2} = \frac{\lambda}{N} \frac{\hbar^2 \rho^2}{m} |qpq_1q_2|^{1/2}$  in the above expression. The fact that the momentum of three of the phonons have same sign and the fourth one has the opposite sign makes the product of all four wave numbers negative. Thus substituting

$$|qpq_1q_2| = -qpq_1q_2 \quad (4.103)$$

and simplifying the expression, we get

$$\delta j_E^I = \alpha \sum_{q^+ p^- q_1^- q_2^-} \hbar\omega_q qpq_1q_2 \delta_{p, q_1+q_2} \delta\left(q + \frac{3}{2} \xi q_1 q_2 p\right) g_p g_{q_1} g_{q_2}, \quad (4.104)$$

$$\text{where } \alpha = -(d-c)(c+d)^3 \frac{\delta T}{T} \frac{1}{2s} \left[ \frac{\lambda}{N} \frac{\hbar^2 \rho^2}{m} \right]^2 \left[ \frac{2\pi}{\hbar^2} \right]. \quad (4.105)$$

*Dirac and Kronecker delta functions*

We first sum over  $p$  which gets rid of the Kronecker delta function and results in the following expression

$$\delta j_E^I = \alpha \sum_{q^+ q_1^- q_2^-} \hbar \omega_q q (q_1 + q_2) q_1 q_2 \delta(q + \frac{3}{2} \xi q_1 q_2 (q_1 + q_2)) g_{q_1 + q_2} g_{q_1} g_{q_2}. \quad (4.106)$$

This is the ideal time to go from a sum over discrete values of momenta to continuous integrals. We use relation 4.23 and simplify to get the integral form:

$$\delta j_E^I = \alpha \left( \frac{L}{2\pi} \right)^3 \int_0^\infty dq \int_{-\infty}^0 dq_1 \int_{-\infty}^0 dq_2 \hbar \omega_q q (q_1 + q_2) q_1 q_2 \delta(q + \frac{3}{2} \xi q_1 q_2 (q_1 + q_2)) g_{q_1 + q_2} g_{q_1} g_{q_2} \quad (4.107)$$

$$\delta j_E^I = \alpha \left( \frac{L}{2\pi} \right)^3 \int_{-\infty}^0 dq_1 \int_{-\infty}^0 dq_2 \hbar \omega_{-\frac{3}{2} \xi q_1 q_2 (q_1 + q_2)} \left( -\frac{3}{2} \xi q_1 q_2 (q_1 + q_2) \right) (q_1 + q_2) q_1 q_2 g_{q_1 + q_2} g_{q_1} g_{q_2} \quad (4.108)$$

$$\delta j_E^I = \alpha \left( \frac{3\xi}{2} \right)^2 \hbar s \left( \frac{L}{2\pi} \right)^3 \int_{-\infty}^0 dq_1 \int_{-\infty}^0 dq_2 \frac{q_1^3}{2 \sinh(\hbar \omega_{q_1}/2T)} \frac{q_2^3}{2 \sinh(\hbar \omega_{q_2}/2T)} \frac{(q_1 + q_2)^3}{2 \sinh(\hbar \omega_{q_1 + q_2}/2T)} \quad (4.109)$$

$$\delta j_E^I = \alpha \left( \frac{3\xi}{2} \right)^2 \hbar s \left( \frac{L}{2\pi} \right)^3 \int_{-\infty}^0 dq_1 \int_{-\infty}^0 dq_2 \frac{q_1^3}{2 \sinh(\hbar \omega_{q_1}/2T)} \frac{q_2^3}{2 \sinh(\hbar \omega_{q_2}/2T)} \frac{(q_1 + q_2)^3}{2 \sinh(\hbar \omega_{q_1 + q_2}/2T)}. \quad (4.110)$$

To extract the leading term in wavenumbers  $q_1$  and  $q_2$ , we can approximate  $\omega(q) \approx s|q|$ :

$$\delta j_E^I = \alpha \left( \frac{3\xi}{2} \right)^2 \hbar s \left( \frac{L}{2\pi} \right)^3 \int_{-\infty}^0 dq_1 \int_{-\infty}^0 dq_2 \frac{q_1^3}{2 \sinh(\hbar |q_1| s/2T)} \frac{q_2^3}{2 \sinh(\hbar s |q_2|/2T)} \frac{(q_1 + q_2)^3}{2 \sinh(\hbar s |q_1 + q_2|/2T)} \quad (4.111)$$

Since  $q_1 < 0 \Rightarrow |q_1| = -q_1$  and  $q_2 < 0 \Rightarrow |q_2| = -q_2$ . Further, we can make the substi-

tution  $q_1 = 2Tx/\hbar s$  and  $q_2 = 2Ty/\hbar s$  to bring the integral in dimensionless form,

$$\delta j_E^I = -\frac{\alpha}{2^3} \left(\frac{3\xi}{2}\right)^2 \hbar s \left(\frac{L}{2\pi}\right)^3 \left[\frac{2T}{\hbar s}\right]^{11} \int_{-\infty}^0 dx \int_{-\infty}^0 dy \frac{x^3}{\sinh x} \frac{y^3}{\sinh y} \frac{(x+y)^3}{\sinh(x+y)}. \quad (4.112)$$

Due to indistinguishability of  $q_1$  and  $q_2$ , actual  $\delta j_E^I$  is half the calculated value.

$$\delta j_E^I = -\frac{1}{2^3} \frac{4}{\kappa(1+\kappa^2)^2} \frac{\delta T}{T} \left[\frac{1}{2s}\right] \left[\frac{\lambda}{N} \frac{\hbar^2 \rho^2}{m}\right]^2 \left[\frac{2\pi}{\hbar^2}\right] \left[ \left(\frac{3\xi}{2}\right)^2 \hbar s \left(\frac{L}{2\pi}\right)^3 \left[\frac{2T}{\hbar s}\right]^{11} \frac{4\pi^{10}}{3465} \right] \quad (4.113)$$

Similarly, the remaining contributions can be calculated upto  $T^8$  term. But being equal and opposite, these contribution cancel out making the leading order in temperarue contributions as: Here  $\delta j_E^{III}$  and  $\delta j_E^{IV}$  originate from the same scattering process, so only one of them will contribute to total current. The  $T^{10}$  terms for  $\delta j_E^{II}$  and  $\delta j_E^{III}$  the leading powers in temperature. The three corrections are:

$$\delta K^I = -\frac{3^2 \beta_I}{2^5} \frac{4}{\kappa(1+\kappa^2)^2} \left(\frac{\xi^2}{s}\right) \left[\frac{\lambda}{N} \frac{\hbar^2 \rho^2}{m}\right]^2 \left[\frac{2\pi}{\hbar^2}\right] \left(\frac{2T}{\hbar s}\right)^{10} \left(\frac{L}{2\pi}\right)^3 \quad (4.114)$$

$$\delta K^{II} = -\frac{3\beta_{II}}{2^5} \frac{4}{\kappa(1+\kappa^2)^2} \left(\frac{\xi^2}{s}\right) \left[\frac{\lambda}{N} \frac{\hbar^2 \rho^2}{m}\right]^2 \left[\frac{2\pi}{\hbar^2}\right] \left(\frac{2T}{\hbar s}\right)^{10} \left(\frac{L}{2\pi}\right)^3 \quad (4.115)$$

$$\delta K^{III} = \frac{3\beta_{III}}{2^4} \frac{4}{\kappa(1+\kappa^2)^2} \left(\frac{\xi^2}{s}\right) \left[\frac{\lambda}{N} \frac{\hbar^2 \rho^2}{m}\right]^2 \left[\frac{2\pi}{\hbar^2}\right] \left(\frac{2T}{\hbar s}\right)^{10} \left(\frac{L}{2\pi}\right)^3 \quad (4.116)$$

The constants  $\beta_I$ ,  $\beta_{II}$  and  $\beta_{III}$  are:

$$\beta_I = \int_{-\infty}^0 \int_{-\infty}^0 dx dy \frac{x^3}{\sinh x} \frac{y^3}{\sinh y} \frac{(x+y)^3}{\sinh(x+y)} = \frac{4\pi^{10}}{3465} \quad (4.117)$$

$$\beta_{II} = \int_0^\infty \int_0^\infty dx dy \frac{x^2}{\sinh x} \frac{y^2}{\sinh y} \frac{(x+y)^5}{\sinh(x+y)} = 516.90 \quad (4.118)$$

$$\beta_{III} = \int_0^\infty \int_0^\infty dx dy \frac{x^5}{\sinh x} \frac{y^2}{\sinh y} \frac{(x+y)^2}{\sinh(x+y)} = 96.29 \quad (4.119)$$

#### 4.9.1 Result

The net correction to thermal conductance is the sum of all three contribution  $\delta K = \delta K^I + \delta K^{II} + \delta K^{III}$

$$\delta K = -243.241 \times \left( \frac{1}{\kappa(1+\kappa^2)^2} \left( \frac{\xi^2}{s} \right) \left[ \frac{\lambda}{N} \frac{\hbar^2 \rho^2}{m} \right]^2 \left[ \frac{2\pi}{\hbar^2} \right] \left( \frac{2T}{\hbar s} \right)^{10} \left( \frac{L}{2\pi} \right)^3 \right) \quad (4.120)$$

Here  $\kappa = q/k = v_F \rho / s$  is the Luttinger liquid parameter of the one-dimensional electron liquid. Since  $K_0 = \frac{\pi T}{6\hbar}$ ,

$$\frac{\delta K}{K_0} \propto T^9$$

## CHAPTER 5

### RESULTS AND DISCUSSION

The main result of our work is the calculation of correction to the thermal conductance of a one-dimensional Wigner crystal quantum wire in a relatively realistic one-dimensional quantum wire setup 4.6.

Luttinger liquid theory is the one-dimensional equivalent of Fermi liquid theory [23] in the sense that it explains key physical properties of many-particle systems with weak and strong interactions.

The Luttinger liquid Hamiltonian:

$$H_0 = \sum_k \hbar \omega_k b_k^\dagger b_k, \quad (5.1)$$

has bosonic excitations with a linear dispersion. This is the fixed point Hamiltonian in the renormalization group framework and is sufficient to account for the power-law correlations in one-dimensional systems. However, it does not describe lifetime of bosonic excitations and thermalization of boson distribution function. A theory needs presence of interaction and scattering between its excitations to account for such effects. Therefore, a real quantum wire lies beyond the applicability of Luttinger liquid theory.

A one-dimensional Wigner crystal is an ideal model to study the effects of transition to non-linearity. At low temperatures and sufficiently rapidly decaying interaction potential (faster than  $1/x$ ), a harmonic Wigner crystal is essentially an extreme limit of Luttinger liquid. Under linear approximation, our calculation for thermal conductance for a clean harmonic one-dimensional Wigner crystal of *spinless* electrons gave the result:

$$K_0 = \frac{\pi T}{6\hbar}. \quad (5.2)$$

It is interesting to note that the thermal conductance  $K_0$  calculated here is exactly the same as reported for non-interacting electrons [87, 15]. This is a pure Luttinger liquid result with bosons travelling ballistically without any interaction with each other or the homogenous medium.

The above result can be thought of as a zeroth order approximation to the thermal conductance of a Wigner crystal wire. It also reaffirms the validity of Luttinger liquid theory for ideal cases. However, the violation of Wiedemann-Franz law in experimental studies inspires us to try to extend the Luttinger liquid theory beyond linear bosonic excitations to study its thermal and electrical transport coefficients.

### 5.1 Correction to thermal conductance

Two primary sources of change in transport coefficients are, (i) backscattering of phonons due to inhomogeneity in Wigner crystal [15], and (ii) redistribution of energy due to scattering between phonons (bosonic excitations). In this thesis, we study the effect of interaction on thermal conductance. We introduced interaction by considering the cubic and quartic anharmonic perturbations of the Wigner crystal. This leads to divergences in the presence of a linear dispersion of phonons. Therefore, we introduced a weak non-linearity parametrized by  $\xi$  to successfully resolve the divergences. A non-linear dispersion does not allow decay of a phonon into two phonons. The leading non-zero contribution comes from the four particle scattering term. For a weak non-linearity, the dominant scattering processes have scattering of two co-moving phonons into a final state where a parametrically small momentum and energy is back scattered. This class of scattering processes resolve the divergences and result in a finite rate of scattering.

The phonon backscattering was introduced by considering the changing width of the electron channel as is the case in real 2DEG based quantum point contacts 1.2. Our result for the relative correction to thermal conductance  $\delta K/K_0$  due to these two new contribu-

tions is:

$$\frac{\delta K}{K_0} = -CN \frac{\rho}{\kappa(1 + \kappa^2)^2} \frac{\hbar^2 \xi^2 \lambda^2}{m^2 s^2} \left( \frac{T}{\hbar s} \right)^9, \quad (5.3)$$

where

$$C = 243.241 \frac{3 \times 2^{10}}{\pi^3}.$$

Our result is valid for a Wigner crystal, i.e., strongly interacting electrons. Therefore, the Luttinger liquid parameter is small and positive

$$0 < \kappa \ll 1.$$

In this limit, our result in equation (5.3) simplifies to:

$$\boxed{\frac{\delta K}{K_0} = -CN \frac{\rho^4 \hbar^2 \xi^2 \lambda^2}{\kappa m^2 s^2} \left( \frac{T}{\hbar s} \right)^9} \quad (5.4)$$

Here  $\kappa = q/k = v_F \rho / s$  is the Luttinger liquid parameter of the one-dimensional electron liquid. Since  $K_0 = \frac{\pi T}{6\hbar}$ ,

$$\frac{\delta K}{K_0} \propto T^9$$

## 5.2 Fate of Wiedemann-Franz law

As discussed in section 1.2.2, an ideal Luttinger liquid satisfies the Wiedemann-Franz law. However, in the extreme limit  $0 < \kappa \ll 1$ , Luttinger liquid forms a Wigner crystal. The correction to electrical conductance  $G_0 = e^2/h$  in a Wigner crystals originates in the slowest scattering process called *umklapp* scattering 4.5.1. Matveev *et al.* showed that the conductance correction [84] is exponential in temperature:

$$\delta G/G_0 \propto -N e^{-\hbar\omega_\pi/T} \quad (5.5)$$

However, scattering between acoustic phonons  $|q| \ll \pi$  conserve the quasimomentum

and results in no correction to the electrical conductance. Moreover, our results show that the thermal conductance correction due to phonon-phonon scattering and inhomogeneity backscattering is power-law in temperature. Thus, the different temperature dependence of corrections to  $G_0$  and  $K_0$  leads to the breakdown of Wiedemann-Franz law already in the first order in length of the wire  $N$ .

### 5.2.1 Applicability to integral models

Our result for thermal conductance correction has been calculated with a general inter-electron interaction  $V(x)$ .  $\lambda$  and  $\xi$  and  $s$  parametrize the type of interaction. For example, let us consider the integrable models [24] which do not undergo relaxation even in the presence of collisions. This is because they have conservation laws that forbid redistribution of momentum. The Toda lattice model and Calogero-Sutherland have the interaction potential

$$V(x) = \frac{V_0}{\sinh^2(cx)}. \quad (5.6)$$

The parameter  $\lambda$  vanishes for integrable model and therefore the correction to thermal conductance  $\delta K$  for these models vanishes. This is what we expect for integrable models.

### 5.2.2 Screened Coulomb interaction

Another realistic case is the screened Coulomb interaction:

$$V(x) = \begin{cases} \frac{e^2}{x}, & x \ll d \\ \frac{4e^2 d^2}{|x^3|}, & x \gg d \end{cases}$$

in the case of two-dimensional electron gas device based Wigner crystal wire. For this case the parameter  $\lambda = 3/4$  [55]. Thus the problem is reduced to calculating the relevant parameters to be used in our expression for  $\delta K$ .

### 5.2.3 Comparison with weakly interacting electrons

Although weakly interacting electrons are also described as Luttinger liquids, it is noteworthy that their correction to thermal conductance as calculated in [88],

$$\delta K_{weak} \propto T^6 \quad \text{weak interaction,}$$

is different from the Wigner crystal case ( $\delta_{WC} \propto T^{10}$ ). This is due to the leading non-linearity in the dispersion relation in the two cases. While the non-linear deviation is a cubic order in momentum for a Wigner crystal, it is square order for weakly interacting electrons. We expect that at very low temperatures the  $T^{10}$  dependence will crossover to  $T^6$ . Investigating the crossover behavior is an interesting problem and can be the subject of future work.

Our estimate of the conductance correction is valid in the classical regime where temperature is high,  $T \gg vp_*$ , and bosons are the good excitations. We expect the electron description regime, where  $T \ll vp_*$ , to have a correction  $\delta K(T)$  to be similar to that found by Levchenko *et al.* [88]. For weakly interacting electrons, they solved the Boltzmann equation for three electron scattering process and found the correction to be proportional to  $T^2$ :

$$\delta K(L) \propto -LT^2, \quad l_a \ll L \ll l_b \quad (5.7)$$

$$\delta K(L) \propto -T^2, \quad l_a \ll l_b \ll L \ll l_{eq}. \quad (5.8)$$

Here,  $l_a$  is the intra-branch inelastic scattering length for three particle collision,  $L$  is the length of the wire,  $l_b$  is the inter-branch three particle scattering length and  $l_{eq}$  is the exponentially large ( $\sim e^{\mu/T}$ ) equilibration length that represents complete equilibration between left and right movers [88]. Our current estimates lack the accuracy to verify whether the quantum and classical asymptotes for  $\delta K(T)$  match for the quantum to classical crossover

region where  $T \sim p_*$ . We expect that the crossover from quantum ( $T \ll \nu p_*$ ) to classical ( $T \gg \nu p_*$ ) regime should be smooth and featureless.

# Appendices

**APPENDIX A**  
**INTEGRALS**

This integral was part of a scattering problem to find the conductance of a one dimensional boson gas.

$$f(x) = \frac{x^3}{\sinh(x)}$$

$$I = \int_0^\infty \int_0^\infty dx dy f(x) f(y) f(x+y)$$

We know that  $f(x) = f(-x)$ . Now, let  $z=x+y$ ,

$$I = \int_0^\infty \int_0^\infty \int_0^\infty dx dy dz f(x) f(y) f(z) \delta(x+y-z)$$

$$I = \int_0^\infty \int_0^\infty \int_{-\infty}^0 dx dy dz f(x) f(y) f(z) \delta(x+y+z)$$

The required integral is a surface integral over the plane  $x + y + z = 0$  and the plane lies entirely in only six of the octants. (It cannot go into the regions  $x > 0, y > 0, z > 0$  and  $x < 0, y < 0, z < 0$ .) Thus, the required integral is one sixth of the integral calculated over all 3-d space.

$$I = \frac{I_{allspace}}{6}$$

$$\begin{aligned}
I &= \frac{1}{6} \int_{-\infty}^{\infty} \int_{-\infty}^{\infty} \int_{-\infty}^{\infty} dx dy dz f(x) f(y) f(z) \delta(x+y+z) \\
&= \frac{1}{6} \int_{-\infty}^{\infty} \int_{-\infty}^{\infty} \int_{-\infty}^{\infty} dx dy dz f(x) f(y) f(x+y) \left[ \frac{1}{2\pi} \int_{-\infty}^{\infty} d\omega e^{i\omega(x+y+z)} \right] \\
&= \frac{1}{6} \frac{1}{2\pi} \int_{-\infty}^{\infty} d\omega \int_{-\infty}^{\infty} dx f(x) e^{i\omega x} \int_{-\infty}^{\infty} dy f(y) e^{i\omega y} \int_{-\infty}^{\infty} dz f(z) e^{i\omega z} \\
&= \frac{(2\pi)^2}{6} \int_{-\infty}^{\infty} d\omega (\tilde{f}(\omega))^3 \\
&= \frac{4\pi^{10}}{3465} = 108.107414\dots
\end{aligned}$$

where  $\tilde{f}(x)$  is the fourier transform of  $f(x)$ ,

$$\tilde{f}(\omega) = \frac{1}{2\pi} \int_{-\infty}^{\infty} dx f(x) e^{i\omega x}$$

## REFERENCES

- [1] L. Esaki and R. Tsu, “Superlattice and Negative Differential Conductivity in Semiconductors,” *IBM Journal of Research and Development*, vol. 14, no. 1, pp. 61–65, Jan. 1970.
- [2] T. Ando and H. Fukuyama, “Quantum Transport in Mesoscopic Systems: An Introduction,” in *Transport Phenomena in Mesoscopic Systems*, H. Fukuyama and T. Ando, Eds., ser. Springer Series in Solid-State Sciences, Berlin, Heidelberg: Springer, 1992, pp. 3–24, ISBN: 978-3-642-84818-6.
- [3] F. Capasso and G. Margaritondo, Eds., *Heterojunction Band Discontinuities: Physics and Device Applications*. Amsterdam ; New York : New York, NY, USA: North-Holland ; Sole distributors for the USA and Canada, Elsevier Science Pub. Co, 1987, ISBN: 978-0-444-87060-5.
- [4] G. Bastard, *Wave Mechanics Applied to Semiconductor Heterostructures*. Les Ulis Cedex, France; New York, N.Y.: Les Editions de Physique ; Halsted Press, 1988, OCLC: 20591224, ISBN: 978-0-470-21708-5 978-2-86883-092-0.
- [5] B. J. van Wees, H. van Houten, C. W. J. Beenakker, J. G. Williamson, L. P. Kouwenhoven, D. van der Marel, and C. T. Foxon, “Quantized conductance of point contacts in a two-dimensional electron gas,” *Physical Review Letters*, vol. 60, no. 9, pp. 848–850, Feb. 1988.
- [6] D. A. Wharam, T. J. Thornton, R. Newbury, M. Pepper, H. Ahmed, J. E. F. Frost, D. G. Hasko, D. C. Peacock, D. A. Ritchie, and G. A. C. Jones, “One-dimensional transport and the quantisation of the ballistic resistance,” *Journal of Physics C: Solid State Physics*, vol. 21, no. 8, pp. L209–L214, Mar. 1988.
- [7] G. V. Chester and A. Thellung, “The Law of Wiedemann and Franz,” *Proceedings of the Physical Society*, vol. 77, no. 5, pp. 1005–1013, May 1961.
- [8] G. Catelani and I. L. Aleiner, “Interaction corrections to thermal transport coefficients in disordered metals: The quantum kinetic equation approach,” *Journal of Experimental and Theoretical Physics*, vol. 100, no. 2, pp. 331–369, Feb. 2005.
- [9] A. L. Éfros and M. Pollak, *Electron-Electron Interactions in Disordered Systems*. North-Holland Publ., 1985, ISBN: 978-0-444-86916-6.
- [10] J. Voit, “One-Dimensional Fermi liquids,” *Reports on Progress in Physics*, vol. 58, no. 9, pp. 977–1116, Sep. 1995. arXiv: cond-mat/9510014.

- [11] T. Giamarchi, *Quantum Physics in One Dimension*. Clarendon Oxford, 2004.
- [12] D. L. Maslov and M. Stone, “Landauer conductance of Luttinger liquids with leads,” *Physical Review B*, vol. 52, no. 8, R5539–R5542, Aug. 1995.
- [13] I. Safi and H. J. Schulz, “Transport in an inhomogeneous interacting one-dimensional system,” *Physical Review B*, vol. 52, no. 24, R17040–R17043, Dec. 1995.
- [14] V. V. Ponomarenko, “Renormalization of the one-dimensional conductance in the Luttinger-liquid model,” *Physical Review B*, vol. 52, no. 12, R8666–R8667, Sep. 1995.
- [15] R. Fazio, F. W. J. Hekking, and D. E. Khmelnitskii, “Anomalous Thermal Transport in Quantum Wires,” *Physical Review Letters*, vol. 80, no. 25, pp. 5611–5614, Jun. 1998.
- [16] M. Pustilnik, M. Khodas, A. Kamenev, and L. I. Glazman, “Dynamic Response of One-Dimensional Interacting Fermions,” *Physical Review Letters*, vol. 96, no. 19, p. 196 405, May 2006.
- [17] A. M. Lunde, K. Flensberg, and L. I. Glazman, “Three-particle collisions in quantum wires: Corrections to thermopower and conductance,” *Physical Review B*, vol. 75, no. 24, p. 245 418, Jun. 2007.
- [18] G. A. Fiete, “Colloquium: The spin-incoherent luttinger liquid,” *Reviews of Modern Physics*, vol. 79, no. 3, pp. 801–820, JUL-SEP 2007, WOS:000248867000001.
- [19] J. S. Meyer and K. A. Matveev, “Wigner crystal physics in quantum wires,” *Journal of Physics: Condensed Matter*, vol. 21, no. 2, p. 023 203, 2009.
- [20] J. Rech, T. Micklitz, and K. A. Matveev, “Conductance of Fully Equilibrated Quantum Wires,” *Physical Review Letters*, vol. 102, no. 11, p. 116 402, Mar. 2009.
- [21] M. Pustilnik, E. Mishchenko, L. Glazman, and A. Andreev, “Coulomb Drag by Small Momentum Transfer between Quantum Wires,” *Physical Review Letters*, vol. 91, no. 12, p. 126 805, Sep. 2003.
- [22] C. L. Kane and M. P. A. Fisher, “Transport in a one-channel Luttinger liquid,” *Physical Review Letters*, vol. 68, no. 8, pp. 1220–1223, Feb. 1992.
- [23] L. Landau, “Zh Eksperim. i Theor Fiz. 30 1058 (1956),” *ENGLISH TRANSLATION: Soviet. Phys. JEPT*, vol. 3, no. 920, p. 164, 1956.

- [24] B. Sutherland, *Beautiful Models: 70 Years of Exactly Solved Quantum Many-Body Problems*, Fir edition. River Edge, N.J: World Scientific Pub Co Inc, Sep. 2004, ISBN: 978-981-238-897-1.
- [25] H. Bethe, “Zur Theorie der Metalle,” *Zeitschrift für Physik*, vol. 71, no. 3, pp. 205–226, Mar. 1931.
- [26] S.-i. Tomonaga, “Remarks on Bloch’s Method of Sound Waves applied to Many-Fermion Problems,” *Progress of Theoretical Physics*, vol. 5, no. 4, pp. 544–569, Jan. 1950.
- [27] J. M. Luttinger, “An Exactly Soluble Model of a Many Fermion System,” *Journal of Mathematical Physics*, vol. 4, no. 9, pp. 1154–1162, Sep. 1963.
- [28] F. Bloch, “Bremsvermögen von Atomen mit mehreren Elektronen,” *Zeitschrift für Physik*, vol. 81, no. 5-6, pp. 363–376, 1933.
- [29] F. Bloch, “Inkohärente Röntgenstreuung und Dichteschwankungen eines entarteten Fermigases,” *Helv. Phys. Acta*, vol. 7, pp. 385–405, 1934.
- [30] R. Shankar, “Bosonization: How to make it work for you in condensed matter,” *Acta Phys.Polon.*, vol. B26, pp. 1835–1867, 1995.
- [31] K. Schonhammer, “Luttinger Liquids: The Basic Concepts,” *arXiv:cond-mat/0305035*, May 2003. arXiv: cond-mat/0305035.
- [32] D. C. Mattis and E. H. Lieb, “Exact Solution of a Many-Fermion System and Its Associated Boson Field,” *Journal of Mathematical Physics*, vol. 6, no. 2, pp. 304–312, Feb. 1965.
- [33] F. D. M. Haldane, “‘Luttinger liquid theory’ of one-dimensional quantum fluids. I. Properties of the Luttinger model and their extension to the general 1D interacting spinless Fermi gas,” *Journal of Physics C: Solid State Physics*, vol. 14, no. 19, pp. 2585–2609, Jul. 1981.
- [34] F. D. M. Haldane, “General Relation of Correlation Exponents and Spectral Properties of One-Dimensional Fermi Systems: Application to the Anisotropic  $S=1/2$  Heisenberg Chain,” *Physical Review Letters*, vol. 45, no. 16, pp. 1358–1362, Oct. 1980.
- [35] ———, “Effective harmonic-fluid approach to low-energy properties of one-dimensional quantum fluids,” *Physical Review Letters*, vol. 47, no. 25, pp. 1840–1843, Dec. 1981.

- [36] E. Wigner, “On the Interaction of Electrons in Metals,” *Physical Review*, vol. 46, no. 11, pp. 1002–1011, Dec. 1934.
- [37] L. I. Glazman, I. M. Ruzin, and B. I. Shklovskii, “Quantum transport and pinning of a one-dimensional Wigner crystal,” *Physical Review B*, vol. 45, no. 15, pp. 8454–8463, Apr. 1992.
- [38] H. J. Schulz, “Wigner crystal in one dimension,” *Physical Review Letters*, vol. 71, no. 12, pp. 1864–1867, Sep. 1993.
- [39] M. Lu, N. Q. Burdick, and B. L. Lev, “Quantum Degenerate Dipolar Fermi Gas,” *Physical Review Letters*, vol. 108, no. 21, p. 215 301, May 2012.
- [40] I. Bloch, J. Dalibard, and W. Zwerger, “Many-body physics with ultracold gases,” *Reviews of Modern Physics*, vol. 80, no. 3, pp. 885–964, Jul. 2008.
- [41] R. Grimm, M. Weidemüller, and Y. B. Ovchinnikov, “Optical Dipole Traps for Neutral Atoms,” in *Advances In Atomic, Molecular, and Optical Physics*, B. Bederson and H. Walther, Eds., vol. 42, Academic Press, Jan. 2000, pp. 95–170.
- [42] Z. Hadzibabic, S. Stock, B. Battelier, V. Bretin, and J. Dalibard, “Interference of an Array of Independent Bose-Einstein Condensates,” *Physical Review Letters*, vol. 93, no. 18, p. 180 403, Oct. 2004.
- [43] T. Kinoshita, T. Wenger, and D. S. Weiss, “Observation of a One-Dimensional Tonks-Girardeau Gas,” *Science*, vol. 305, no. 5687, pp. 1125–1128, Aug. 2004.
- [44] B. Paredes, P. Fedichev, J. I. Cirac, and P. Zoller, “ $\frac{1}{2}$ -Anyons in Small Atomic Bose-Einstein Condensates,” *Physical Review Letters*, vol. 87, no. 1, p. 010 402, Jun. 2001.
- [45] M. P. A. Fisher and L. I. Glazman, “Transport in a one-dimensional Luttinger liquid,” *arXiv:cond-mat/9610037*, Oct. 1996. arXiv: cond-mat / 9610037.
- [46] A. M. Chang, “Chiral Luttinger liquids at the fractional quantum Hall edge,” *Reviews of Modern Physics*, vol. 75, no. 4, pp. 1449–1505, Nov. 2003.
- [47] M. Bockrath, D. H. Cobden, J. Lu, A. G. Rinzler, R. E. Smalley, L. Balents, and P. L. McEuen, “Luttinger-liquid behaviour in carbon nanotubes,” *Nature*, vol. 397, no. 6720, p. 598, Feb. 1999.
- [48] Z. Yao, H. W. C. Postma, L. Balents, and C. Dekker, “Carbon nanotube intramolecular junctions,” *Nature*, vol. 402, no. 6759, p. 273, Nov. 1999.

- [49] A. J. Schwartz, M. Dressel, G. P. Gruner, V. Vescoli, L. Degiorgi, T. G. Ucla, ETH-Zurich, and UPS-Orsay, “On-chain electrodynamics of metallic (TMTSF)<sub>2</sub>X salts: Observation of Tomonaga-Luttinger liquid response,” 1998.
- [50] O. M. Auslaender, A. Yacoby, R. de Picciotto, K. W. Baldwin, L. N. Pfeiffer, and K. W. West, “Tunneling Spectroscopy of the Elementary Excitations in a One-Dimensional Wire,” *Science*, vol. 295, no. 5556, pp. 825–828, Jan. 2002.
- [51] V. V. Deshpande and M. Bockrath, “The one-dimensional Wigner crystal in carbon nanotubes,” *Nature Physics*, vol. 4, no. 4, pp. 314–318, Apr. 2008.
- [52] J. Cao, Q. Wang, and H. Dai, “Electron transport in very clean, as-grown suspended carbon nanotubes,” *Nature Materials*, vol. 4, no. 10, p. 745, Oct. 2005.
- [53] W. K. Hew, K. J. Thomas, M. Pepper, I. Farrer, D. Anderson, G. A. C. Jones, and D. A. Ritchie, “Incipient Formation of an Electron Lattice in a Weakly Confined Quantum Wire,” *Physical Review Letters*, vol. 102, no. 5, p. 056 804, Feb. 2009.
- [54] A. Imambekov, T. L. Schmidt, and L. I. Glazman, “One-dimensional quantum liquids: Beyond the Luttinger liquid paradigm,” *Reviews of Modern Physics*, vol. 84, no. 3, pp. 1253–1306, Sep. 2012.
- [55] J. Lin, K. A. Matveev, and M. Pustilnik, “Thermalization of Acoustic Excitations in a Strongly Interacting One-Dimensional Quantum Liquid,” *Physical Review Letters*, vol. 110, no. 1, p. 016 401, Jan. 2013.
- [56] M. Khodas, A. Kamenev, and L. I. Glazman, “Photosolitonic effect,” *Physical Review A*, vol. 78, no. 5, p. 053 630, Nov. 2008.
- [57] G. E. Astrakharchik and L. P. Pitaevskii, “Lieb’s soliton-like excitations in harmonic traps,” *EPL (Europhysics Letters)*, vol. 102, no. 3, p. 30 004, 2013.
- [58] M. Pustilnik and K. A. Matveev, “Low-energy excitations of a one-dimensional Bose gas with weak contact repulsion,” *Physical Review B*, vol. 89, no. 10, p. 100 504, Mar. 2014.
- [59] I. V. Protopopov, D. B. Gutman, M. Oldenburg, and A. D. Mirlin, “Dissipationless kinetics of one-dimensional interacting fermions,” *Physical Review B*, vol. 89, no. 16, p. 161 104, Apr. 2014.
- [60] M. Pustilnik and K. A. Matveev, “Solitons in a one-dimensional Wigner crystal,” *Physical Review B*, vol. 91, no. 16, p. 165 416, Apr. 2015.
- [61] —, “Fate of classical solitons in one-dimensional quantum systems,” *Physical Review B*, vol. 92, no. 19, p. 195 146, Nov. 2015.

- [62] J. Devreese, *Highly Conducting One-Dimensional Solids*. Springer US, 1979, ISBN: 978-0-306-40099-5.
- [63] J. Sólyom, “The Fermi gas model of one-dimensional conductors,” *Advances in Physics*, vol. 28, no. 2, pp. 201–303, Apr. 1979.
- [64] E. H. Lieb and F. Y. Wu, “Absence of Mott Transition in an Exact Solution of the Short-Range, One-Band Model in One Dimension,” *Physical Review Letters*, vol. 20, no. 25, pp. 1445–1448, Jun. 1968.
- [65] H. J. Schulz, “Correlation exponents and the metal-insulator transition in the one-dimensional Hubbard model,” *Physical Review Letters*, vol. 64, no. 23, pp. 2831–2834, Jun. 1990.
- [66] A. R. Goñi, A. Pinczuk, J. S. Weiner, J. M. Calleja, B. S. Dennis, L. N. Pfeiffer, and K. W. West, “One-dimensional plasmon dispersion and dispersionless intersubband excitations in GaAs quantum wires,” *Physical Review Letters*, vol. 67, no. 23, pp. 3298–3301, Dec. 1991.
- [67] K. Schwab, E. A. Henriksen, J. M. Worlock, and M. L. Roukes, “Measurement of the quantum of thermal conductance,” *Nature*, vol. 404, no. 6781, pp. 974–977, Apr. 2000.
- [68] O. Chiatti, J. T. Nicholls, Y. Y. Proskuryakov, N. Lumpkin, I. Farrer, and D. A. Ritchie, “Quantum Thermal Conductance of Electrons in a One-Dimensional Wire,” *Physical Review Letters*, vol. 97, no. 5, p. 056 601, Aug. 2006.
- [69] J. T. Nicholls and O. Chiatti, “Thermal measurements of a one-dimensional wire in the quantum limit,” *Journal of Physics: Condensed Matter*, vol. 20, no. 16, p. 164 210, Apr. 2008.
- [70] F. Sfigakis, A. C. Graham, K. J. Thomas, M. Pepper, C. J. B. Ford, and D. A. Ritchie, “Spin effects in one-dimensional systems,” *Journal of Physics: Condensed Matter*, vol. 20, no. 16, p. 164 213, Apr. 2008.
- [71] G. Granger, J. P. Eisenstein, and J. L. Reno, “Observation of Chiral Heat Transport in the Quantum Hall Regime,” *Physical Review Letters*, vol. 102, no. 8, p. 086 803, Feb. 2009.
- [72] C. Altimiras, H. le Sueur, U. Gennser, A. Cavanna, D. Mailly, and F. Pierre, “Non-equilibrium edge-channel spectroscopy in the integer quantum Hall regime,” *Nature Physics*, vol. 6, no. 1, pp. 34–39, Jan. 2010.

- [73] Y.-F. Chen, T. Dirks, G. Al-Zoubi, N. O. Birge, and N. Mason, “Nonequilibrium Tunneling Spectroscopy in Carbon Nanotubes,” *Physical Review Letters*, vol. 102, no. 3, p. 036 804, Jan. 2009.
- [74] G. Barak, H. Steinberg, L. N. Pfeiffer, K. W. West, L. Glazman, F. von Oppen, and A. Yacoby, “Interacting electrons in one dimension beyond the Luttinger-liquid limit,” *Nature Physics*, vol. 6, no. 7, pp. 489–493, Jul. 2010.
- [75] C. Kittel, *Introduction to Solid State Physics*, 8 edition. Hoboken, NJ: Wiley, Nov. 2004, ISBN: 978-0-471-41526-8.
- [76] N. W. Ashcroft and N. D. Mermin, *Solid State Physics*, 1 edition. New York: Brooks Cole, Jan. 1976, ISBN: 978-0-03-083993-1.
- [77] E. M. Lifshitz and L. P. Pitaevskii, *Statistical Physics: Theory of the Condensed State*. Oxford: Butterworth-Heinemann, Jan. 1980, ISBN: 978-0-7506-2636-1.
- [78] J. M. Ziman, *Principles of the Theory of Solids*. Cambridge University Press, 1972, ISBN: 978-0-521-29733-2.
- [79] R. D. Mattuck, *A Guide to Feynman Diagrams in the Many-Body Problem*. Courier Corporation, Jan. 1992, ISBN: 978-0-486-67047-8.
- [80] K. V. Samokhin, “Lifetime of excitations in a clean Luttinger liquid,” *Journal of Physics: Condensed Matter*, vol. 10, no. 31, pp. L533–L538, Aug. 1998.
- [81] M. Yamamoto, M. Stopa, Y. Tokura, Y. Hirayama, and S. Tarucha, “Coulomb drag between quantum wires: Magnetic field effects and negative anomaly,” *Physica E: Low-dimensional Systems and Nanostructures*, Proceedings of the Fourteenth International Conference on the Electronic Properties of Two-Dimensional Systems, vol. 12, no. 1–4, pp. 726–729, Jan. 2002.
- [82] P. Debray, V. N. Zverev, V. Gurevich, R. Klesse, and R. S. Newrock, “Coulomb drag between ballistic one-dimensional electron systems,” *Semiconductor Science and Technology*, vol. 17, no. 11, R21, 2002.
- [83] D. Laroche, G. Gervais, M. P. Lilly, and J. L. Reno, “Positive and negative Coulomb drag in vertically integrated one-dimensional quantum wires,” *Nature Nanotechnology*, vol. 6, no. 12, pp. 793–797, Dec. 2011.
- [84] K. A. Matveev, A. V. Andreev, and M. Pustilnik, “Equilibration of a One-Dimensional Wigner Crystal,” *Physical Review Letters*, vol. 105, no. 4, p. 046 401, Jul. 2010.

- [85] A. Gramada and M. E. Raikh, “Tunneling into a periodically modulated Luttinger liquid,” *Physical Review B*, vol. 55, no. 3, pp. 1661–1666, Jan. 1997.
- [86] L. P. Pitaevskii and E. M. Lifshitz, *Physical Kinetics*. Butterworth-Heinemann, Dec. 2012, ISBN: 978-0-08-057049-5.
- [87] L. G. C. Rego and G. Kirczenow, “Quantized Thermal Conductance of Dielectric Quantum Wires,” *Physical Review Letters*, vol. 81, no. 1, pp. 232–235, Jul. 1998.
- [88] A. Levchenko, T. Micklitz, Z. Ristivojevic, and K. A. Matveev, “Interaction effects on thermal transport in quantum wires,” *Physical Review B*, vol. 84, no. 11, p. 115 447, Sep. 2011.

## VITA

Kamal Sharma was born in 1986 in Kota, a town in the state of Rajasthan in north-west India. He graduated with a bachelors degree in civil engineering from Indian Institute of Technology Roorkee. After working for about a year in Tata Consulting Engineers Ltd. as a structural engineer in training, he joined Raman Research Institute as a visiting student in the theoretical Physics group under Prof. Narendra Kumar and Prof. Arun Roy. He joined the School of Physics at Georgia Institute of Technology in Atlanta, Georgia as a PhD student in 2012 where he worked with Prof. Michael Pustilnik as his advisor on transport in one-dimensional interacting systems.